SGU Rapporter och meddelanden 137

Rapporter och meddelanden 137

Past shore-level and sea-level displacements

Tore Påsse & Johan Daniels

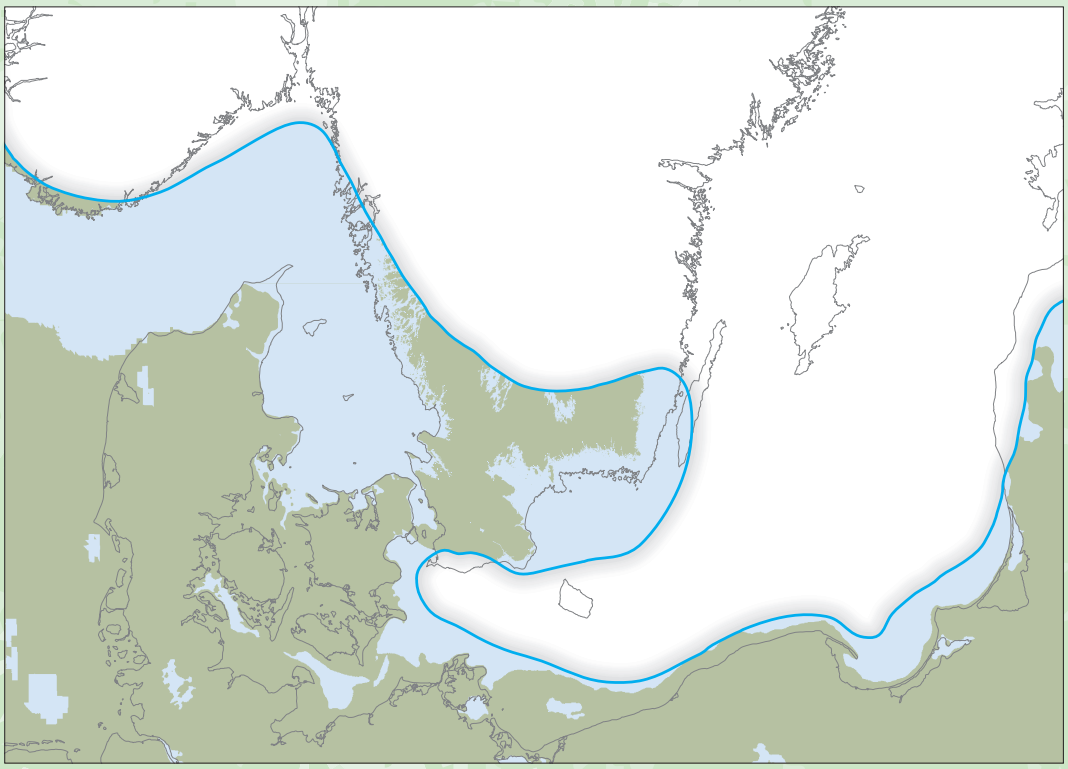

Past shore-level and sea-level displacements

SGU
Sveriges geologiska undersökning
Geological Survey of Sweden

Rapporter och meddelanden 137

Past shore-level and sea-level displacements

Tore Påsse & Johan Daniels

Sveriges geologiska undersökning
2015

ISSN 0349-2176
ISBN 978-91-7403-291-8

Cover: Paleogeograpical map showing the distribution of land (green), ice (white) and sea and lakes (blue). This map was constructed by the model presented in this paper.

Layout: Rebecca Litzell
Tryck: Elanders Sverige AB

Contents

Sammanfattning

Strandförskjutningen och landhöjningsförloppet i Skandinavien har beräknats från empiriska data. Beräkningarna har gjorts utgående från 92 strandförskjutningskurvor, fyra detaljerade sjöstjälpningskurvor, 1 150 HK-värden och mätserier från 57 pegelstationer. Denna modellering är den enda som gjorts med hjälp av empirisk landhöjningsinformation. Genom tillgång till landhöjningsdata har det globala eustatiska förloppet kunnat beräknas med relativt stor noggrannhet. Havsnivåns förändringar beror på två komponenter, dels den huvudsakliga havsytehöjningen, dels en oscillatorisk komponent som skapat små förändringar mellan höjningar och sänkningar. Periodiciteten för oscillationerna är ca 550 år. Båda komponenterna styrs av klimatet.

Nyckelord: Havsytehöjning, landhöjning, strandförskjutning, strandnivåkartor

Abstract

Shore-level displacement and glacio-isostatic uplift in the area affected by the Scandinavian ice sheet have been calculated using empirical data. The calculations are based on 92 shore-level curves from Scandinavia, four detailed lake-tilting investigations, 1 150 levels of the highest coastline, and 57 tide-gauge data. This is the only shore-level model based on empirical data on the crustal uplift. Since the uplift process is known from a source other than sea-level data, it has been possible to calculate global eustatic development within the model. Eustatic development comprises two movements: the main eustatic rise and an oscillatory movement, which have created small changes between rises and falls in sea-level. Both these movements essentially mirror climate trends. The periodicity of the oscillations is approximately 550 years.

Key words: eustasy, glacio-isostasy, shore-level displacement, land uplift, paleogeography.

Introduction

Shore-level displacement is caused by two interactive movements: local crustal depression or uplift and global eustatic sea-level lowering or rise. This paper presents a model for calculating these movements.

After the Weichselian glaciation, which culminated around 21 000 BP, water that had been locked in continental ice sheets returned to the global ocean. The melting of the great ice sheets caused the isostatically depressed crust to elevate as pressure on it lessened. At the same time the ocean bottom sank when glacial meltwater entered the ocean, causing the continental margins to tilt upwards – a result of hydro-isostatic levering. According to Walcott (1972), there are three sea-level regions:

1. Large uplift under the melting ice sheet.
2. Submergence peripheral to the ice sheets.
3. Coastal tilting causing the emergence of continental shorelines distant from the ice.

The interaction of sea-level rise and crustal rise has thus produced a regionally variable shore-level displacement history, making it difficult to isolate eustatic changes.

Fennoscandia, especially Sweden, has outstanding conditions for shore-level investigations. Most shorelines formed during the late Weichselian and Holocene are situated above the present sea-level. There is a greater density of shore-level data in Scandinavia than anywhere else in the world. Lakes, suitable for constructing shore-level curves, are abundant in the region. More than 1 000 highest coastline sites, between 20 and 285 m above present sea-level, are reported within Sweden. There are practically no tides along the west coast of Sweden or in the Baltic Sea. The tidal range is normally less than 5 cm. Sea-level observations have been performed in Stockholm since 1774, and this record is one of the longest continuous sea-level series in the world.

Whitehouse (2009) has presented a detailed review of the current understanding of glacial-isostatic adjustment developed by leading researchers in this field. There are two methods for modelling shore-level displacement. The most common is to model shore-level displacement by combining information on the geophysical structure of the Earth with information on the evolution of surface loading from dated shorelines and ice-sheet reconstructions (Cathles 1975, Fjeldskaar 1994, 2000, Fjeldskaar & Cathles 1991, Lambeck 1991, 1997, 1999, McConnel 1968, Peltier 1974, 1976). Most of these studies focus on analysing the isostatic mechanism. Variations in the volume and distribution of ice are the principal cause of sea-level change. Information on temporal and spatial evolution of ice sheets must be very accurate for the creation of a detailed model of glacial-isostatic change from geophysical modelling. Such information does not exist at present.

An alternative method of modelling shore-level displacement, used in this paper, is to analyse exclusively empirical shore-level data with spatial statistics and mathematical calculations (Påsse 1996a, 1997, 2001, Påsse & Andersson 2005, Påsse & Daniels 2011). The main focus of this research is to achieve better knowledge of shore-level displacement in areas where empirical data do not exist, but also to achieve better knowledge of eustatic changes.

The shore-level model

EMPIRICAL DATA

We have developed our shore-level model using empirical data from four sources: lake-tilting data, shore-level curves, tide gauge data and elevations of the highest coastline. The positions of the data sets are shown in Figure 1.

Lake-tilting data show the difference in uplift between the sampling sites and the outlets. The lake-tilting method is an outstanding tool for modelling glacio-isostatic movements, as the data do not include eustatic changes, and the course of glacio-isostatic uplift can be described using numerical estimates alone.

Detailed studies of glacio-isostatically induced tilting of four lakes in southern Sweden have been presented by Påsse (1990a, 1996b, 1998). An example of this is shown in Figure 2.

The primary information used in shore-level modelling is shore-level curves representing continuous sets of data. 92 shore-level curves from the area covered by Scandinavian ice during the Late Weichselian are used

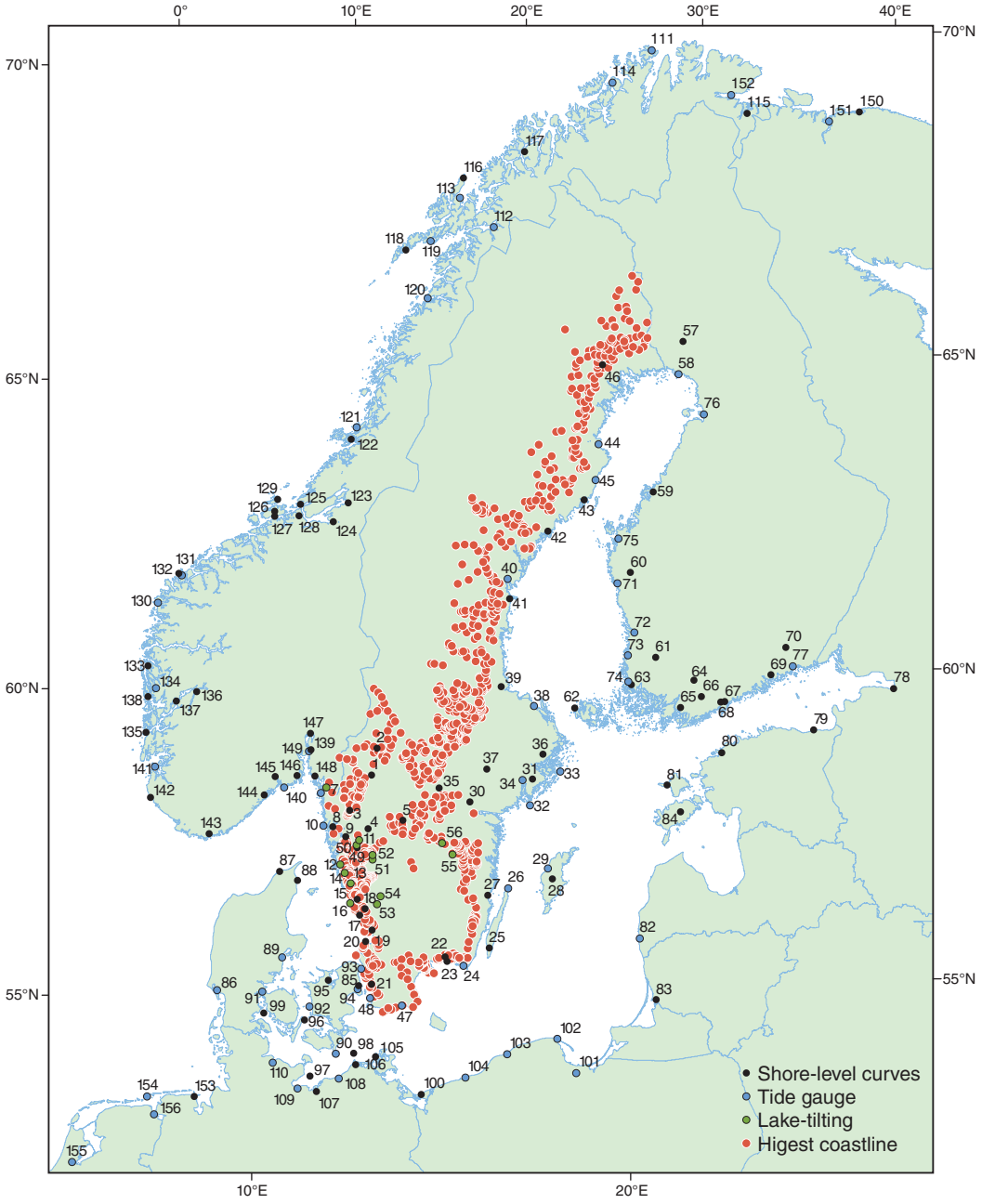

Figure 1. Position of shore-level curves, tide gauges, tilted lakes and highest coastlines used in the modelling. Numbers refer to Table 1, where names of sites and references are listed.

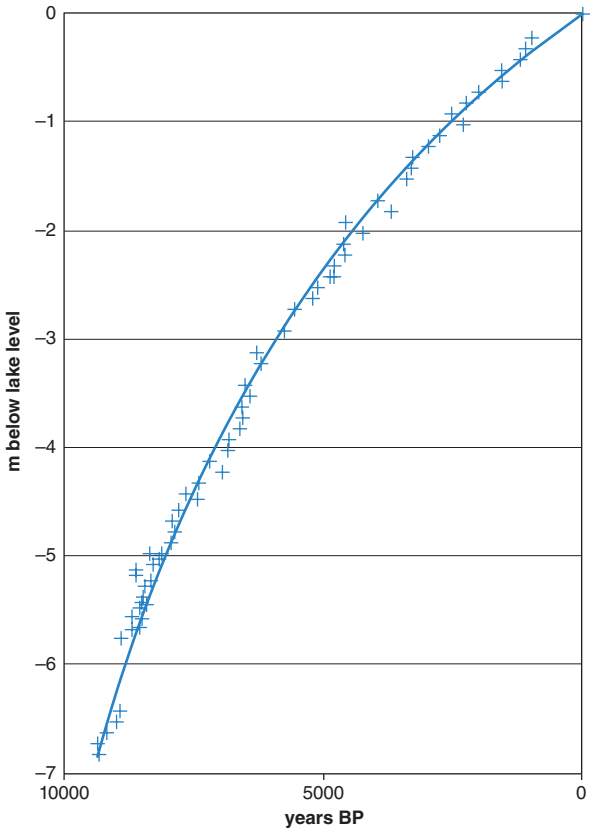

Figure 2. Radiocarbon dates (plus signs) for ancient lake levels in the lake Sommen (Påsse 1990a, 1996a). The curve shows the difference in land uplift between the outlet in the north and the southern part of the lake.

as input data for the modelling. The position of each sea-level site is presented in Figure 1 and the references for these curves are reported in Table 1. Vuorela (2009) has presented a summary and revision of Finnish shore-level data, which is used in this paper.

When using shore-level curves for modelling, it is important to understand that the accuracy of most assessments of the curves is somewhat uncertain. Shore-level curves are constructed from data relating to time and level. The main source of error derives from collecting data over too large an area. The assessment of the shore-level therefore has a fairly large margin of error. Other problems associated with shore-level curves are that the material used in the dating comes from very different sources and that those sources seldom relate to an exact shore-level position.

For the uninitiated shore-level researcher, it may seem as though the biggest source of dating error is that many shore-level curves are dated by pollen analyses. However, particularly for curves representing the late Weichselian, dating precision is much better using pollen analytical dates than radiocarbon dates alone. Another source of error is the problem of dating an exact shore-level. For example, what does the date of a twig found in clay represent?

Shore-level curves are rarely constructed from single accurate ^{14}C dates. Usually it is sediment above or beneath a horizon that is dated. Notwithstanding all these sources of error, shore-level curves provide the only information useful for building the framework for shore-level modelling. The advantage of using shore-level curves instead of single dates is that the data for constructing the curves have been evaluated for all possible errors. Using single dates in the modelling may look more scientific in diagrams, but may actually create more problems than advantages.

Most sea-level curves relate the information to a conventional ^{14}C scale. However, in this work, it is necessary to use a calendar scale to calculate the time-dependent uplift, which means that many scales have been converted into calendar scales.

Harald Agrell, of the Geological Survey of Sweden, has compiled a highest coastline database. It comprises more than 1 150 sites, each evaluated in detail. Shore-level data consist of four dimensions, position (x, y), elevation (y) and time (t). It is possible to calculate the age of the highest coastline by modelling, since this coastline is formed during deglaciation. The highest coastline has been used in the model to extend the spatial distribution of shore-level information. The positions of the sites are shown in Figure 1.

Digital information on most tide gauge stations in the world is accessible at http://www.psmsl.org./data/obtaining. This information has been compiled by Woodworth & Player (2003). The tide gauge zero level is calibrated by analysing the data set in relation to nearby tide gauge data series, where local meteorological variation can be assumed to be similar. The data sets can thus be adjusted fairly well in line with local variations.

Tide gauge data are used in two ways within the model. Similarly to the use of the highest coastline, the tide gauge data have been used to extend the spatial distribution of shore-level information and also to obtain information on present eustatic development. The positions of the 57 tide gauges used in the model are presented in Figure 1.

METHOD

The present model is a further development of the shore-level models presented by Påsse (1996a, 1997, 2001) and by Påsse & Andersson (2005). An extended model for shore-level development throughout the Weichselian glaciation has also been presented by Morén & Påsse (2001). Like previous models, the present model started by combining the results from empirical lake-

Table 1. Numbers, names, coordinates in Sweref 90 TM and references of the sites used in the calculations. The model variables *A* (m), *T* (years BP), B_e (years) and B_v (years) given the best correlation between theoretical and empirical shore-level curves are reported in the table. The positions of the sites are shown in Figure 1. PSMSL means that the data is from http:\\www.psmsl.org.\data\obtaining.

Nr.	Site	East	North	*A* (m)	*T* (years BP)	B_e (years)	B_v (years)	References
1	A Värmland	370956	6571161	136	11300	1200	7584	Risberg et al. 1996
2	D Värmland	380344	6621250	155	11100	1100	7945	Risberg et al. 1996
3	Kroppefjäll	329769	6505699	109	11600	1600	7071	Björck & Digerfeldt 1991
4	Hunneberg	364165	6471130	101	11700	1700	6919	Björck & Digerfeldt 1982
5	Billingen	428945	6486900	105	11500	1400	6986	Björck & Digerfeldt 1986
6	N Bohuslän	286282	6548149	120	11200	1300	7280	Påsse 2003
7	Strömstad	276410	6538036	113	11200	1300	7147	PSMSL
8	Central Bohuslän	298152	6475336	103	11850	1650	6957	Miller & Robertsson 1988
9	Ljungskile	322362	6456637	98	11900	1650	6862	G. Persson 1973
10	Smögen	281140	6477131	103	11900	1600	6957	PSMSL
11	Risveden	343598	6435903	94	12300	1700	6777	Svedhage 1985
12	Göteborg	311990	6404543	91	13200	1800	6729	Påsse 1983, PSMSL
13	Sandsjöbacka	320175	6388650	88	13350	1800	6672	Påsse 1987
14	Fjärås	331393	6369794	85	13400	1700	6615	Påsse 1986
15	Varberg West	330832	6332808	73	13500	1600	6387	Påsse 1990b, PSMSL
16	Varberg East	343740	6339957	77	13450	1600	6454	M. Berglund 1995
17	Falkenberg West	348091	6310025	69	13600	1400	6311	Påsse 1988
18	Falkenberg East	358942	6322147	72	13550	1400	6359	Påsse 1988
19	Halmstad	371406	6282315	66	13600	1350	6245	Caldenius & Linman 1949
20	Bjäre Peninsula	359660	6261188	65	13900	1150	6226	Mörner 1980
21	Barsebäck	370588	6181358	48	14000	900	5893	Digerfeldt 1975, G. Persson 1962, Ringberg 1989
22	Blekinge	507925	6232939	56,5	13200	1700	6074	Björck 1979, Björck & Möller 1987
23	Blekinge	511029	6223978	53,5	13250	1700	6017	Liljegren 1982, Yu et al. 2004
24	Kungsholmsfort	542107	6216344	53	13200	1700	6007	PSMSL
25	Öland	589713	6248892	55	13100	1700	6045	Gembert 1987
26	Öland N	624891	6360280	83	12750	1750	6577	PSMSL
27	Oskarshamn	587548	6347841	74	12700	1750	6406	Svensson 1989
28	Gotland	707164	6378254	72	12500	1700	6368	Svensson 1989
29	Visby	699440	6397160	80	12500	1700	6520	PSMSL
30	Rejmyra	553484	6521385	119	11500	1200	7261	C. Persson 1979
31	Södertälje	651963	6562564	150	11350	1200	7850	PSMSL
32	Landsort	665538	6514736	135	11500	1200	7565	PSMSL
33	Grönskär	722761	6578418	150	11400	1200	7850	PSMSL
34	Stockholm	670945	6563793	148	11350	1200	7812	Åse 1970, Miller & Robertsson 1982, Brunnberg et al. 1985, Risberg 1991, Hedenström & Risberg 1999, PSMSL
35	Närke	496186	6547686	134	11350	1200	7546	Hedenström 2001, Hedenström & Risberg 2003
36	Tärnan	690382	6610022	152	11350	1200	7888	Hedenström 2001, Hedenström & Risberg 2003
37	Eskilstuna	585734	6582758	151	11200	1200	7869	Robertsson 1991
38	Forsmark	673290	6699799	165	11250	1400	8135	PSMSL
39	Gästrikland	611857	6736039	175	11100	1500	8325	Berglund 2005, 2010
40	Spikarna	624363	6937148	213	10600	1900	9047	PSMSL
41	Hälsingland	627823	6900199	202	10700	1600	8838	Lundqvist 1962
42	Ångermanland	699234	7026070	224	10600	1900	9256	Cato 1992, Berglund 2004
43	S Västerbotten	766484	7084911	225	10600	2000	9275	Renberg & Segerström 1981
44	Furugrund	794169	7188255	229	10600	2000	9351	PSMSL
45	Ratan	788023	7121181	225	10600	2000	9275	PSMSL
46	Norrbotten	801271	7336336	192	10800	1500	8648	Lindén et al. 2006
47	Ystad	427017	6142034	37	13950	1000	5703	PSMSL
48	Malmö	367892	6155341	41	14000	900	5779	PSMSL
49	Vanderyd S	342539	6440887	94	12175	1600	6786	Påsse 1998
50	Vanderyd N	347428	6449941	97	12150	1600	6834	Påsse 1998
51	Säven S	372841	6414264	91	12725	1600	6634	Påsse 1998
52	Säven N	372746	6422258	93	12600	1600	6702	Påsse 1998
53	Fegen S	380833	6330401	78	13100	1600	6482	Påsse 1998

Nr.	Site	East	North	A (m)	T (years BP)	B_e (years)	B_v (years)	References
54	Fegen N	387651	6345474	83	13050	1650	6577	Påsse 1998
55	SommenS	521673	6423035	96	12350	1500	6824	Påsse 1998
56	SommenN	501926	6444292	106	12300	1475	7014	Påsse 1998
57	Rovaniemi	950703	7380265	195	10800	1200	8705	Saarnisto 1981
58	Kemi	942492	7319155	206	10700	1200	8914	PSMSL
59	Kronoby	895295	7099542	207	10600	1300	8933	Vuorela et al. 2009
60	Lauhanwuori	853190	6949008	197	11000	1200	8743	Salomaa 1982, Salomaa & Matiskainen 1983
61	Olkiluoto	900162	6790586	170	11400	1100	8230	Eronen et al. 1995
62	Åland	749318	6696731	165	11250	1400	8135	Glückert 1978
63	Turku	854783	6740024	162	11500	1100	8078	Glückert 1976, Salonen 1984
64	Karjalohka	971690	6748463	123	11600	1000	7337	Glückert & Ristaniemi 1982
65	Tammisaari	946317	6697144	119	11700	1000	7261	Eronen et al. 1995
66	Lohja	985072	6717623	120	11700	1000	7280	Glückert & Ristaniemi 1982
67	Helsinki	1029197	6708163	118	11900	900	7242	Hyvärinen 1980, 1984, Korhola 1995
68	Espo	1021196	6708065	118	11900	900	7242	Glückert & Ristaniemi 1982, Eronen & Haila 1982
69	Porvoo	1114603	6758228	114	12100	900	7166	Eronen 1983
70	Hangassuo	1142976	6809596	114	12100	900	7166	Eronen 1976
71	Kristinestad	828444	6928698	201	11000	1200	8819	PSMSL
72	Pori	860585	6837098	185	11100	1200	8515	PSMSL
73	Rauma	848106	6794942	176	11400	1200	8344	PSMSL
74	Uusikapunki	849710	6745961	167	11400	1200	8173	PSMSL
75	Vaasa	830391	7012721	218	10600	1300	9142	PSMSL
76	Oulu	990464	7243765	206	10600	1200	8914	PSMSL
77	Hamina	1155412	6774738	104	12200	900	6976	PSMSL
78	St. Petersburg	1344013	6733052	45	12400	900	5855	Dolukhanov 1979
79	Narva	1194887	6656179	60	12200	900	6140	Kessel & Raukas 1979
80	Tallin	1023358	6613070	87	12100	900	6653	Kessel & Raukas 1979
81	Köpu	921072	6552819	84	12100	900	6596	Kessel & Raukas 1979
82	Liepaja	870474	6267186	45	13500	900	5855	PSMSL
83	S Lithuania	900817	6152528	32	14000	900	5608	Kabailiené 1997
84	Peispi	946675	6503121	56	12300	900	6064	Rosentau et al. 2008
85	Köpenhamn	344710	6172062	42	14000	900	5798	PSMSL
86	Esbjerg	82913	6171013	0	14000	900	5000	PSMSL
87	Hirtshals	199211	6392207	70	14000	1700	6330	Clemmensen et al. 2001
88	Fredrikshamn	232385	6375614	70	14000	1700	6330	Rickardt 1996, Clemmensen et al. 2001
89	Århus	204109	6231381	45	14000	1000	5855	PSMSL
90	Gedser	304127	6051664	24	14000	900	5456	PSMSL
91	Fredrica	166878	6167994	27	14000	900	5513	PSMSL
92	Korsör	255138	6140041	27	14000	900	5513	PSMSL
93	Hornbaeck	351263	6210117	58	14000	900	6102	PSMSL
94	Vedbäck	346628	6179080	54	14000	900	6026	Christensen 1993
95	Söborg Sö	289541	6189409	51	14000	900	5969	Mörner 1976
96	St Bält	245436	6114946	27	14000	900	5513	Christensen 1993, Bennike & Jensen 1995, Jensen 1999, Bennike et al. 2004
97	W Baltic	255635	6010136	17	14000	900	5323	Winn et al. 1986, Klug 1980
98	Darss sill	337177	6052506	24	14000	900	5456	Bennike & Jensen 1995, Jensen et al. 1999, Bennike et al. 2004
99	Ho bugt	169340	6128054	–2	14000	900	4962	Gehrels et al. 2006
100	Swinemünde	462903	5976519	11	14000	900	5209	Uscinowicz 2003
101	Gdansk	752385	6015898	11	14000	900	5209	PSMSL
102	Wladyslawowo	716659	6079397	17	14000	900	5323	PSMSL
103	Utska	622997	6051325	16	14000	900	5304	PSMSL
104	Kolobrezeg	545520	6007450	13	14000	900	5247	PSMSL
105	Rügen	378143	6046517	29	14000	900	5551	Lampe et al. 2010
106	Fischland	341329	6032103	24	14000	900	5418	Lampe et al. 2010
107	Wismar	267956	5981296	16	14000	900	5304	Lampe et al. 2010, PSMSL
108	Warnemünde	309649	6005756	20	14000	900	5380	PSMSL
109	Travemünde	232916	5986892	10	14000	900	5190	PSMSL

Nr.	Site	East	North	A (m)	T (years BP)	B_e (years)	B_v (years)	References
110	Kiel	186397	6035324	5	14000	900	5095	PSMSL
111	Nordkap	892569	7922501	37	12500	1200	5703	PSMSL
112	Narvik	597975	7592653	124	10700	1200	7356	PSMSL
113	Harstad	535270	7647815	63	12000	1200	6197	PSMSL
114	Hammerfest	819374	7862530	42	12500	1200	5798	PSMSL
115	Kirkenes	1070141	7804866	83	11000	1200	6577	Møller 2003
116	Andöja	541780	7684890	49	13600	1000	5941	Vorren et al. 1988
117	Tromsö	656111	7733385	60	12000	1200	6140	Hald & Vorren 1983, Møller 2003
118	Lofoten	434579	7550530	54	12200	1200	6026	Møller 1984, Vorren & Moe 1986
119	Svolver	480345	7567122	57	12000	1200	6083	PSMSL
120	Bodö	474742	7460087	98	10800	1200	6862	PSMSL
121	Rorvik	342896	7219490	105	10500	1200	6995	PSMSL
122	Näröy	332184	7197364	105	10500	1200	6995	Ramfjord 1982
123	Verdalsöra	326686	7079354	119	10400	1200	7223	Sveian & Olsen 1984
124	Frosta	299147	7044025	105	10400	1200	6995	Kjemperud 1986
125	Bjugn	237775	7076231	77	10600	1200	6463	Kjemperud 1986
126	Hitra	189964	7063634	71	10800	1200	6349	Kjemperud 1986
127	Tjeldbergodden	190090	7053642	71	10800	1200	6349	Solem & Solem 1997
128	Hitra-Heimsjö	235042	7055209	71	10800	1200	6349	Kjemperud 1986
129	Fröja	195681	7085692	58	10800	1200	6102	Kjemperud 1986
130	Malöy	–27723	6893028	43	11800	1200	5817	PSMSL
131	Ålesund	16605	6943540	43	11800	1200	5817	PSMSL
132	Leinöy	11560	6947473	43	11800	1200	5817	Svendsen & Mangerud 1990
133	Fonnes	–46236	6774906	44	10800	1200	5836	Kaland 1984
134	Sotra	–46532	6717956	45	10800	1400	5855	Krzywinski & Stabell 1984, Kaland et al. 1984, Lohne et al. 2007
135	Bömlo	–49706	6650981	42	10800	1300	5798	Kaland 1984
136	Hardanger	44274	6727066	73	10400	500	6387	Helle et al. 1997
137	Törvikbygd	6522	6709617	67	10500	600	6273	Romundset et al. 2010
138	Bergen	–31733	6733124	45	10800	1300	5855	PSMSL
139	Dröback	253482	6615710	146	10850	900	7765	PSMSL
140	Larvik	207332	6548195	101	11100	850	6919	PSMSL
141	Stavanger	–32944	6587246	36	10800	1200	5684	PSMSL
142	Jären	–41243	6530201	36	10800	1200	5684	Thomsen 1981, Bird & Klemsdal 1986
143	Mandal	67473	6462575	39	10800	1200	5732	Midtbö et al. 2000
144	Kragerö	170521	6534759	96	10800	900	6824	Stabell 1980
145	Porsgrunn	191092	6568983	110	10800	800	7090	Stabell 1980
146	Vestfold	232046	6570479	120	11000	950	7280	Sørensen et al. 2012
147	Oslo	257065	6649732	155	10800	800	7950	Hafsten 1983
148	Halden	265032	6569879	124	11000	1300	7356	Sørensen 1999
149	Ski	257443	6618756	147	10850	900	7793	Sørensen 1979
150	Dalnie Zelentsy	1280140	7807664	60	11800	1200	6140	Snyder 1996
151	Polyarniya	1223364	7789903	60	11300	1200	6140	PSMSL
152	Matalaniiemi	1040678	7839477	83	11000	1200	6577	PSMSL
153	N Tyskland	39742	5972699	-2	14000	900	4962	Behre 2007
154	Borkum	–47668	5972701	-4	14000	900	4924	PSMSL
155	Amsterdam	–188108	5850250	-17	14000	900	4677	PSMSL
156	Delfzijl	–35295	5938878	-13	14000	900	4753	PSMSL

tilting research with data from the shore-level curves in an iterative process. These calculations have yielded mathematical formulae for crustal uplift and eustatic rise, which are used to calculate spatial shore-level displacement. Compared to previous models, the present model has been improved by using data from the highest coastline and tide gauge measurements in the modelling process.

FORMULAS FOR LAND UPLIFT

The Earth behaves as an elastic material under short-term stresses and as a fluid under long-term stresses. The modelling in this paper follows the concept, originally used by Nansen (1922), Daly (1934), Cathles (1975) and Peltier & Andrews (1976), that a Maxwell viscoelastic material could be used as a plausible rheological model for explaining glacio-isostatic movements. The behaviour of this material is analogous to an elastic spring together with a viscous dashpot. Nansen (1922) originally described the elastic component as vertical elastic compression and the viscous component as horizontal transport of masses.

In order to simplify treatment of the empirical data in the present model, the empirical shore-level curves are transformed into general mathematical formulae containing as few variables as possible. These general formulae are also used as algorithms to construct paleogeographical maps. A mathematical formula for each shore-level curve is made by fitting the dated points on the curve to a mathematical function. Although hyperparabolic and other mathematical functions could be fitted to these points, arctan functions proved suitable for the following reasons: (1) they match hand-drawn curves better than other functions, (2) they are statistically accurate and (3) they function well in the GIS model. An arctan function can roughly be regarded as a cumulative normal distribution function.

In a previous model (Påsse & Andersson 2005), the calculations of glacio-isostatic uplift were divided into two components which were called the slow and the fast components. Within the present model, these component are named the 'viscous' and the 'elastic' components, respectively.

Land uplift following unloading of ice (U in m) is calculated with the general function:

Formula 1.

$$U = \frac{2}{\pi}\cdot A\cdot\left[\arctan\left\{\frac{T}{B_v}\right\}-\arctan\left\{\frac{T-t}{B_v}\right\}\right]+\frac{2}{\pi}\cdot A\cdot\left[\arctan\left\{\frac{T}{B_e}\right\}-\arctan\left\{\frac{T-t}{B_e}\right\}\right]$$

where A is a down-load factor (m) for the uplift, T (years) is the time for the maximum uplift rate, i.e. the symmetry point of the arctan function, t (year) is the variable time and B_v (y) is the relaxation factor for the viscous uplift. B_e similarly corresponds to the elastic uplift. In the calculations, T and t are counted in calendar years. In this formula there are four unknown variables. In the arctan formula, A defines half the amount to which the function reaches. It is mentioned above as a down-load factor but it could equally have been named half the amount of the total uplift. However, we wish to avoid this latter definition as the formulae are asymptotic, which means that estimations of total uplift only can be made by creating a far end of the duration of uplift. Modelling made it possible to simplify the uplift expression since the relaxation factor for the viscous uplift B_v(y) is related to A (m). B_v(y) is thus calculated from:

Formula 2.

$$B_v = A\cdot 19 + 5000$$

With this simplification the uplift function can be written as:

Formula 3.

$$U = \frac{2}{\pi}\cdot A\cdot\left[\arctan\left\{\frac{T}{A\cdot 19+5000}\right\}-\arctan\left\{\frac{T-t}{A\cdot 19+5000}\right\}\right] + \frac{2}{\pi}\cdot A\cdot\left[\arctan\left\{\frac{T}{B_e}\right\}-\arctan\left\{\frac{T-t}{B_e}\right\}\right]$$

FORMULAE FOR EUSTASY

Eustatic rise is composed of two different movements which are here named the main eustatic rise (E) and the oscillatory factor (Osc). The oscillatory factor caused the sea-level to oscillate in a quasi-regular way superimposed on the main eustatic rise. The main eustatic rise is calculated by:

Formula 4.

$$E = -\frac{2}{\pi}\cdot 29\cdot\left[\arctan\left\{\frac{9200}{1300}\right\}-\arctan\left\{\frac{9200-t}{1300}\right\}\right] - -\frac{2}{\pi}\cdot 36\cdot\left[\arctan\left\{\frac{13700}{1350}\right\}-\arctan\left\{\frac{13700-t}{1350}\right\}\right]$$

where t is in calendar years.
The oscillation factor is calculated by:

Formula 5.

$$Osc = -1.5e^{-0.5\left\{\frac{t-12000^2}{5300}\right\}}\cdot[\sin\{(t-310)\cdot 0.01\}]+0.01$$

The two eustatic formulae are discussed in a later chapter.

WATER LEVEL CHANGES IN THE BALTIC

The accepted model of shore-level development in the Baltic comprises two lake phases: the Baltic Ice Lake and the Ancylus Lake. These two lake phases were

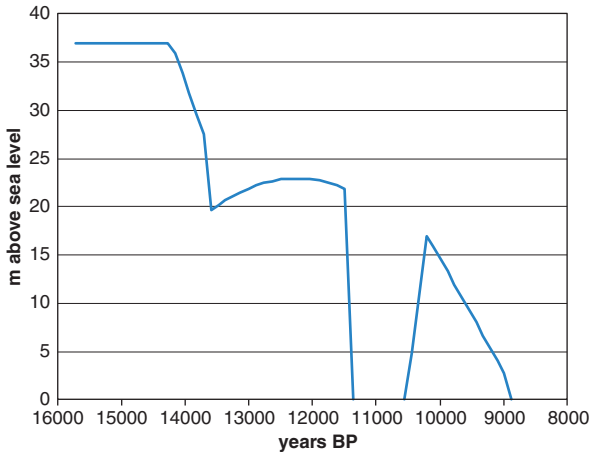

Figure 3. The level of the damming within the Baltic basin during the Baltic Ice Lake and the Ancylus Lake.

each followed by marine phases: the Yoldia Sea and the Littorina Sea. A tentative function that models damming within the Baltic Ice Lake and the Ancylus Lake has been deduced from scarce data within the model (Fig. 3).

The lack of data, particularly on the early phases of the Baltic Ice Lake, is problematic within modelling. For example, the precise location of the outlet of the Baltic Ice Lake prior to the drainage at Billingen has never been positively identified, although most researchers assume that it was in the Öresund Strait. Regarding the relative levels of the Baltic Ice Lake and the relation to the sea, there are actually only three sites with relevant data: Blekinge (Björck 1979, Björck & Möller 1987), Oskarshamn and Gotland (Svensson 1989). Empirical data thus only exist from c. 14 300 BP and onwards, and the relative level of the Baltic Lake before that time is therefore highly uncertain. In this context, it should be emphasised that reliable Late Weichselian shore-level curves do not exist from Denmark and Skåne, and that the model is based solely on postglacial empirical information in that area.

Shorelines in eastern Skåne, conventionally assumed to have been formed at the highest coastline, give some information about the first stages of the Baltic Ice Lake. The levels of these shorelines show that the Baltic Ice Lake must have been dammed about 35–40 m above the sea-level during the initial stage. A glacial lake, the embryonic Baltic Ice Lake, was formed within the Hanö Bay c. 15 700 years BP, when the Low Baltic ice stream protruded into the Öresund and Danish straits. The levels of the sites of the highest coastline in southeastern Skåne can be modelled by a damming of approximately 37 m within the model. This level indicates that the outlet was through the Vomb basin in central Skåne at that time. As the Baltic ice stream receded, the damming gradually decreased. At c. 13 500 years BP the outlet of the Baltic ice went through the present threshold in the Öresund strait, and the damming level followed the shore-level displacement at this site. Initially the damming level was approximately 20 m and ended at around 22 m, before the drainage at Billingen around 11 500 years BP.

The Yoldia Sea existed for one thousand years, between c. 11 500 and c. 10 500 years BP. During this period, the Baltic was connected to the Kattegat Sea by a strait through the Vänern basin. Rapid uplift caused the connection through the Vänern basin to become gradually smaller and shallower. Around 10 500 years BP a threshold was created at Degerfors and the Baltic basin became a lake once more – the Ancylus Lake. For 300 years this lake was tilted towards the south in a huge transgression, the Ancylus transgression. It raised the water level up to 17 m above the sea-level at c. 10 200 years BP, when an outlet was formed within the Danish strait. After this maximum damming the Ancylus Lake became gradually lower and was drained by a river, the Dana River. The level of the Ancylus Lake fell because of the shore-level transgression that occurred in the sea at this time. Approximately 8 900 years BP the sea intruded into the Baltic basin through the Danish strait, and the Baltic once more became an inland sea – the Littorina Sea. Later the sea also intruded through the Öresund strait.

MODELLING USING SHORE-LEVEL CURVES

The uplift trends established within lake-tilting records presented by Påsse (1990a, 1996b, 1998) are exaggerated and used as input data for the crustal uplift in the first iterative calculations. In these calculations, the original data or original hand-drawn shore-level curves are compared to theoretical curves deduced from the formulae presented above. Some of these comparisons are shown in Figures 4–6. The variables A (m), B_e (years) and T (years) with the best correlation between theoretical and empirical shore-level curves were plotted on maps. These variable maps formed the basis for further research.

MODELLING USING DATA ON THE HIGHEST COASTLINE

Each variable map was initially derived using 92 values from coastal sites. The maps were improved within "inland areas" in Sweden using information from the highest coastline.

In most areas, the highest coastline has been formed continuously at the ice border during deglaciation. Because of isostatic uplift, the sea-level regresses imme-

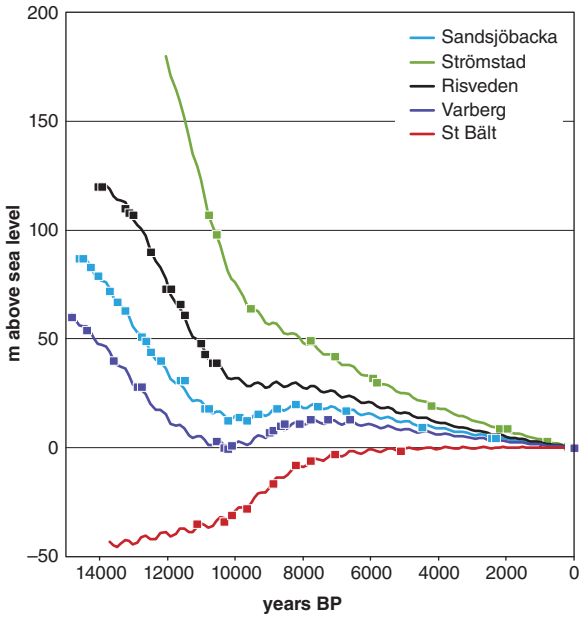

Figure 4. Modelled shore-level curves along a transect from northern Bohuslän at the Swedish west coast, to the Great Belt in Denmark. The squares represent dated shore-levels. For references see Table 1.

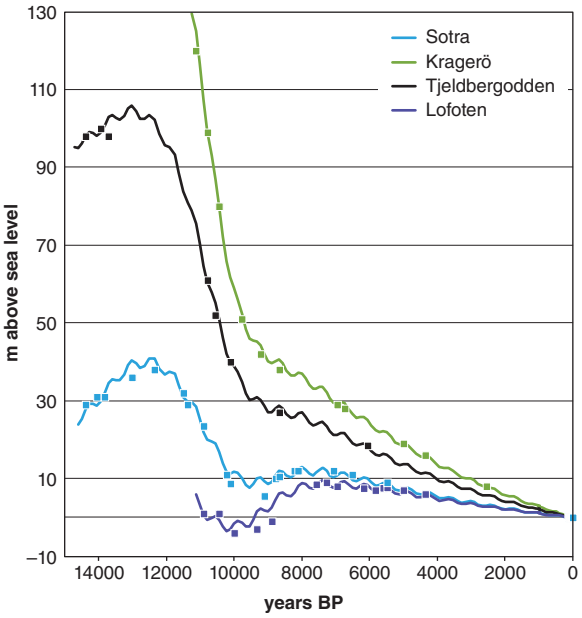

Figure 5. Modelled shore-level curves from the Norwegian West Coast. The squares represent dated shore-levels. For references see Table 1.

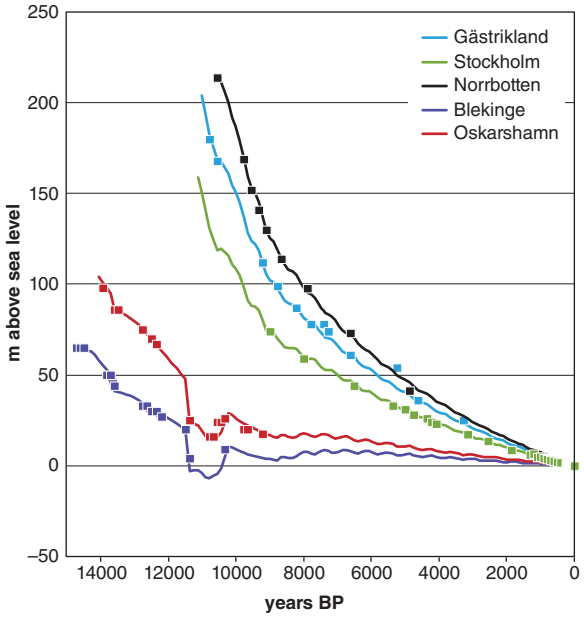

Figure 6. Modelled shore-level curves in a section along the Swedish East Coast. The squares represent dated shore-levels. For references see Table 1.

diately when a site becomes ice free. Thus, the highest shoreline is roughly synchronous with the time of deglaciation. A locality where evidence of the highest shoreline is recorded is a point with latitude, longitude and elevation. When these three parameters are known, the model makes it possible to calculate when the highest coastline was formed at each specific site. The recession of the Scandinavian ice sheet is fairly well known through records presented by Lundqvist (1994), Lundqvist & Wohlfarth (2001) and Andersen et al. (1998). These records make it possible to achieve plausible values for the uplift parameters using the levels of the highest coastline. Each single level within this database, compiled at the Geological Survey of Sweden by H. Agrell, has been transformed into a date, which means that this method also created more than 1 150 new dates of the ice recession. A map with examples of these dates is shown in Figure 7.

MODELLING USING TIDE GAUGE RECORDS

Tide gauge measurements have given several new data points for improving the uplift model, but the most important contribution made by these data is that they helped to improve the eustatic expression. The tide gauges used in the analysis are reported in Table 1. An example of tide gauge records is shown in Figure 8.

The tide gauge zero level is calibrated by analysing the data set in relation to nearby tide gauge series, where

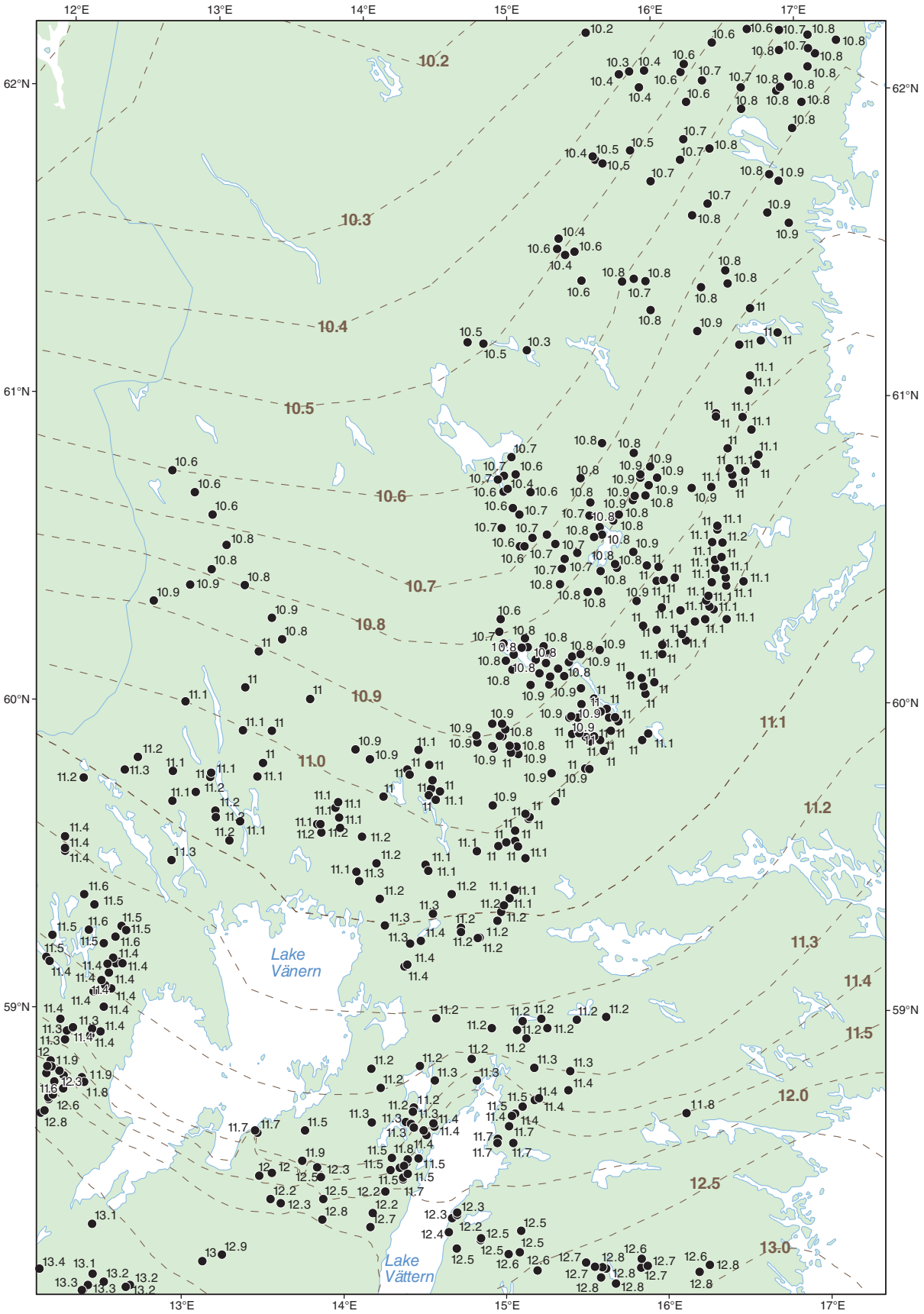

Figure 7. A database with levels of the highest coastline, including more than 1000 sites in Sweden, has been compiled at the Geological Survey of Sweden. Each single level within this database has been transformed to a date by the results of the modelling. A map with examples of these dates is shown in this figure. The dates are written in 1000 years. The dashed lines show ice recession lines partly derived from the dates of the highest coastline.

local meteorological variation can be assumed to be similar. The data sets can thus be fairly well adjusted in line with local variations. This is done by initially calculating the difference between the modelled shore-level displacement and the tide-gauge data. Figure 9 summarises the annual water level variations in Swedish tide gauge records. Similar analyses were made for tide gauge series in Finland and the southern Baltic area, including Denmark and the North Sea. These analyses also make it possible to decide whether the calculated shore-level displacement is correct. If the calculated shore-level were too small or too large, the annual variations would not match the other curves.

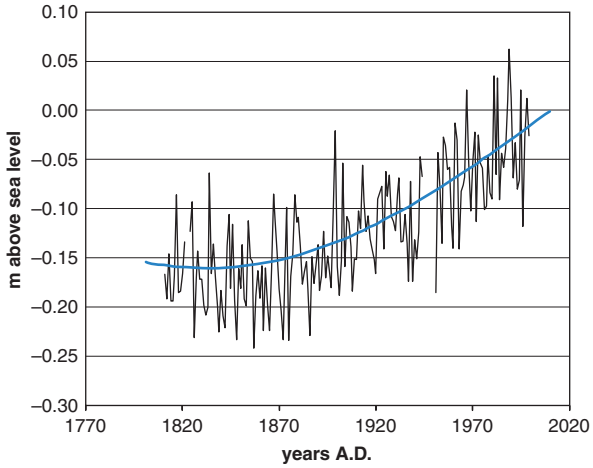

Figure 8. Tide gauge data, black curve, from the Swinemünde station. The blue curve shows the trend of the shore-level displacement derived within the model.

The estimates of the mean meteorological annual variations of the water level within the tide gauge record make it possible to smooth the records by subtracting the mean annual variations from the original records. This analysis is not necessary to obtain a reliable result in the calculations, but it has increased the accuracy in estimating the crustal uplift. Examples of tide gauge records that have been adjusted to the annual variations are shown in Figure 10–11.

The final tide gauge calculations are made by subtracting the tide gauge measurements from the crustal movement established in the model. The result is the present eustatic rise. A mean value curve is calculated for the whole region. The curve is then used to estimate the recent ongoing eustatic rise (Fig. 12). The present ongoing eustatic rise started c. 1820 AD after a period of regression.

STATISTICAL TREATMENT

The outcome of the model consisted of parameter values from tilted lakes, shore-level curves, the highest coastline and tide gauge records. For interpolation of the data points, a minimum curvature technique was used, ensuring a smooth surface, together with continuous first-derivatives. The algorithm generates the smoothest possible surface while honouring the data points. After several iterative calculations, the final values obtained are shown in Figures 13A–D. These maps, together with the formulae, are the main results of the calculations.

TESTING THE MODEL

The models made by Påsse & Andersson (2005) and Påsse & Daniels (2011) used the "recent relative uplift"

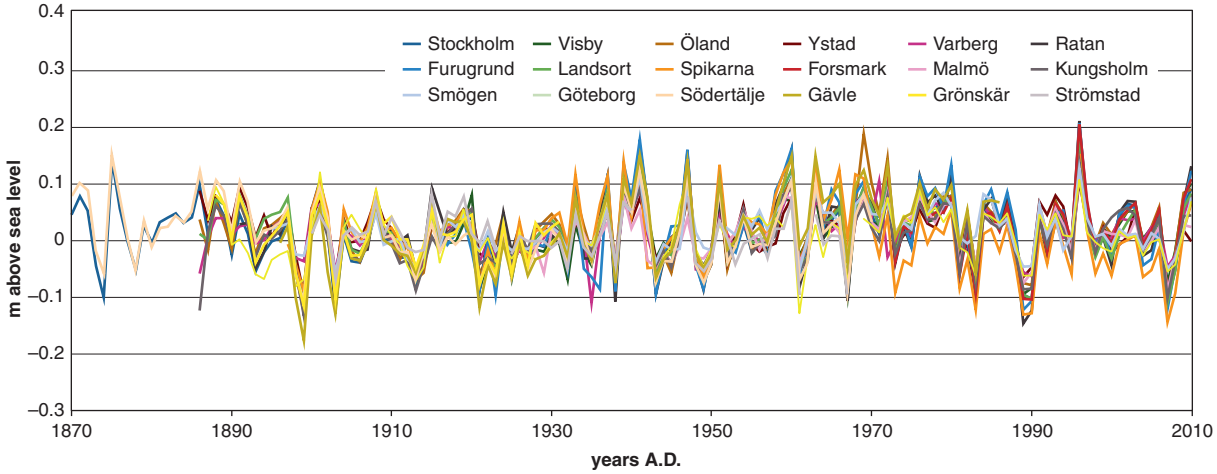

Figure 9. Annual variations within the Swedish tide gauge records that are reported in Table 1.

recorded by precession levelling as input data. The aim of using this information was to extend the data set to inland areas. This information is not used to improve the present model, but instead to test it.

Recent uplift recorded in tide gauge data includes eustatic changes. The shore-level displacement for one year has been calculated in the model, and the configuration of the uplift isolines are compared with isolines received from the "recent relative uplift" (mm/y) described by Ågren & Svensson (2007), RAK (1971) and Ekman (1996). The differences between the values estimated by the shore-level model and the values determined by precision levelling and tide-gauge data is approximately 1.6 mm/y. This figure represents present ongoing eustasy. A present eustatic rise in the order of 1 mm/y has been reported by Lizitzen (1974) and Mörner (1977, 1980), among others. Compilations by Emery & Aubrey (1991), Nakiboglu & Lambeck (1991), Påsse (1996) and Påsse & Andersson (2005) indicate the present rate of eustatic rise to be approximately 1.2 mm/y. Lambeck et al. (1998) and Ekman (2000) estimate the present rise at 1.05 mm/y. All these estimates of present eustatic rise thus give fairly similar results. For observed 20th century sea-level rise, based on tide gauge records, Church (2001) adopted as a best estimate a value of 1 to 2 mm/y.

The modelling results are mainly tested by the configuration of the isolines of the present uplift (Fig. 14). Although the calculated values differ, the trend between the different isolines is fairly consistent. The isolines from the report by Ågren & Svensson (2007) have been smoothed in several steps. These steps include a comparison with a shore-level model by Lambeck (1998). Actually, the correspondence between our testing data and the earlier presented maps of the "recent relative uplift" by RAK (1971) and Ekman (1996) is better, since these two older maps are not as smoothed.

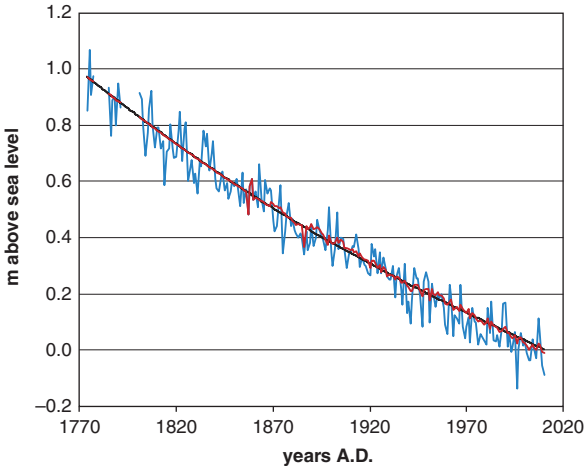

Figure 10. Tide gauge record from Stockholm. The original record is shown by the blue curve while the orange curve is adjusted to the annual variations. The calculated shore-level displacement is shown by the black curve.

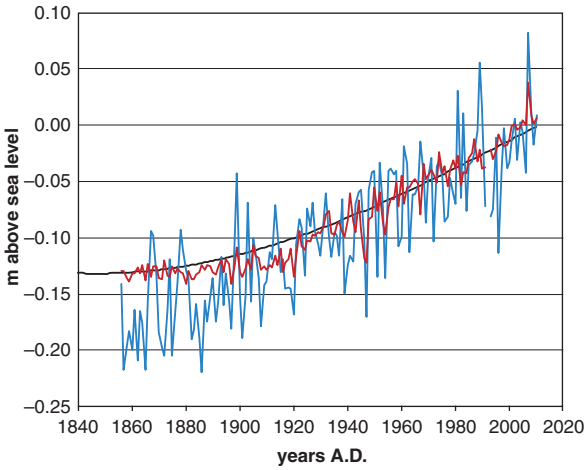

Figure 11. Tide gauge record from Warnemünde in Germany. The original record is shown by the blue curve while the orange curve is adjusted to the annual variations. The calculated shore-level displacement is shown by the black curve. The adjusted curve has a quite different course in the oldest part, which is of utmost importance for the interpretation.

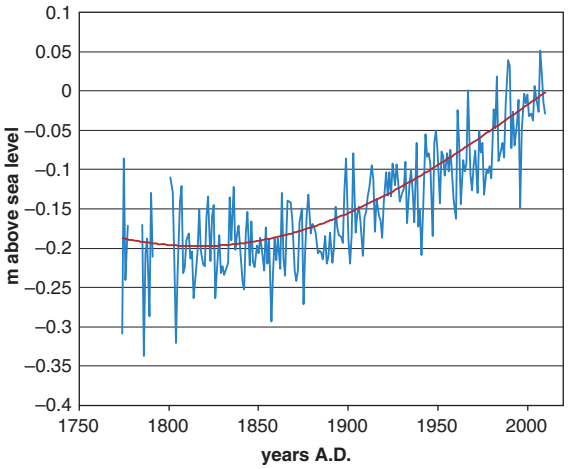

Figure 12. Mean values of the water level changes from tide gauge records corrected for isostatic uplift from sites listed in Table 1. The changes comprise annual changes due to meteorological variations and a small eustatic rise. The red curve shows the calculated eustatic development according to the present model.

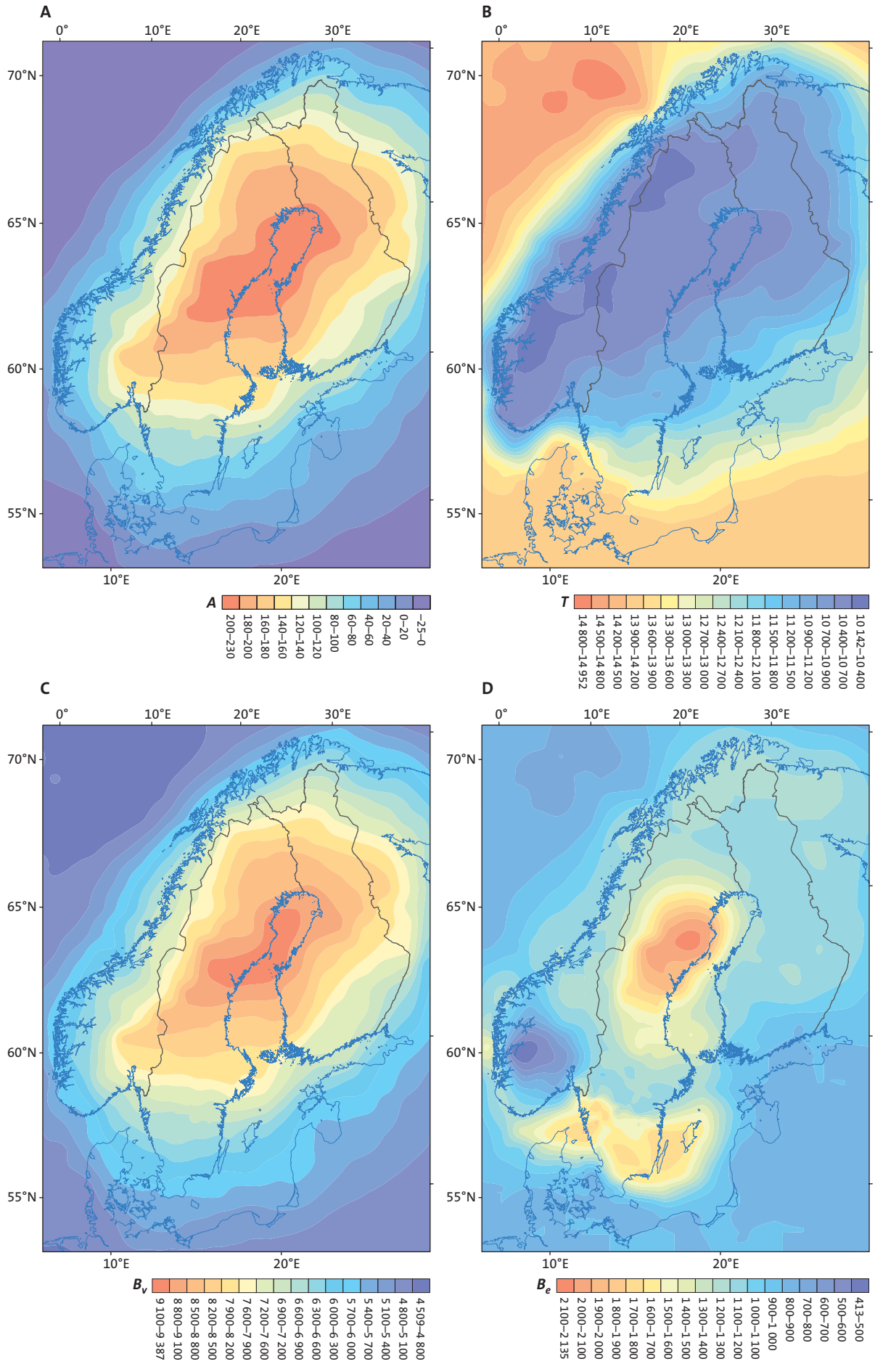
A
0°
10°E
20°E
30°E
70°N
65°N
60°N
55°N
10°E
20°E
A
200–230
180–200
160–180
140–160
120–140
100–120
80–100
60–80
40–60
20–40
0–20
−25–0
B
0°
10°E
20°E
30°E
70°N
65°N
60°N
55°N
10°E
20°E
T
14 800–14 952
14 500–14 800
14 200–14 500
13 900–14 200
13 600–13 900
13 300–13 600
13 000–13 300
12 700–13 000
12 400–12 700
12 100–12 400
11 800–12 100
11 500–11 800
11 200–11 500
10 900–11 200
10 700–10 900
10 400–10 700
10 142–10 400
C
0°
10°E
20°E
30°E
70°N
65°N
60°N
55°N
10°E
20°E
B_v
9 100–9 387
8 800–9 100
8 500–8 800
8 200–8 500
7 900–8 200
7 600–7 900
7 200–7 600
6 900–7 200
6 600–6 900
6 300–6 600
6 000–6 300
5 700–6 000
5 400–5 700
5 100–5 400
4 800–5 100
4 509–4 800
D
0°
10°E
20°E
30°E
70°N
65°N
60°N
55°N
10°E
20°E
B_e
2 100–2 135
2 000–2 100
1 900–2 000
1 800–1 900
1 700–1 800
1 600–1 700
1 500–1 600
1 400–1 500
1 300–1 400
1 200–1 300
1 100–1 200
1 000–1 100
900–1 000
800–900
700–800
600–700
500–600
413–500

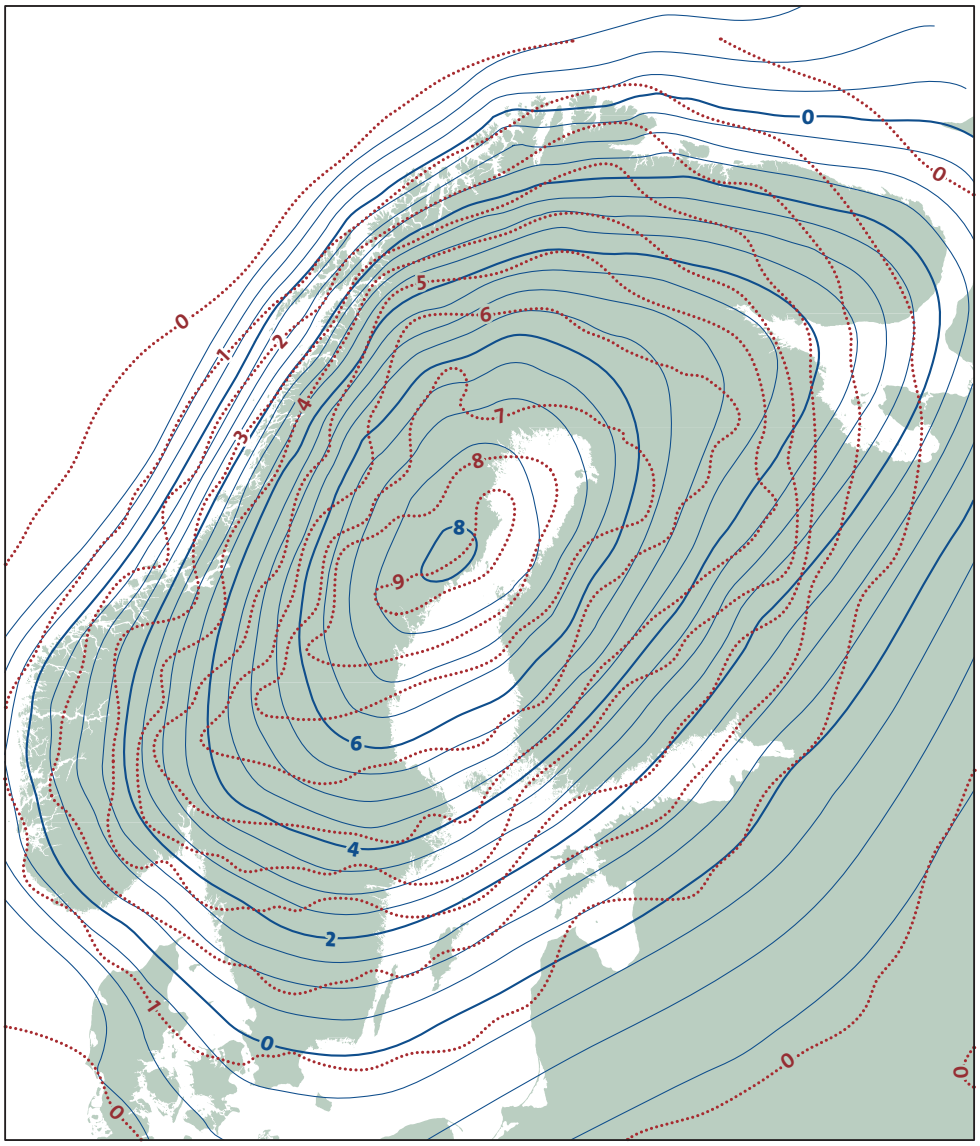

Figure 14. The red isolines show the present uplift for one year calculated by the model. The blue isolines show the present relative uplift according to empirical repeated precision levelling and tide-gauge measurements from Ågren & Svensson (2007). These latter values include eustatic changes so there is a difference of c. 1.6 mm/y between empirical and modelled values. The isolines from Ågren & Svensson (2007) have been smoothed in several steps.

Figure 13. **A.** Map of the variable *A* (m) used in the model. **B.** Map of the variable *T* (years) used in the model. **C.** Map of the variable B_v (years) used in the model. **D.** Map of the variable B_e (years) used in the model.

Results and discussion

THE COURSE OF GLACIO-ISOSTATIC UPLIFT IN SCANDINAVIA

The main trend for maximum uplift is that it occurred in a time-transgressive way following the course of deglaciation. However, there are some exceptions to the main trend. The main uplift in the coastal areas of Norway was delayed and occurred much later than in the rest of Scandinavia. The west coast of Norway was uplifted more or less at the same time as central northern Sweden. This may suggest that thinning of the ice over the Norwegian mountains was very slow relative to the deglaciation of coastal areas. The model actually suggests that the ice cover over Norway should be regarded as a separate glacial system distinguished from the rest of the Scandinavian ice.

The "delay" in the uplift of Norway has given rise to a shore-level development differing from the rest of Scandinavia. Eustatic rise meant that some areas along the west coast of Norway experienced transgression during the initial phase of slow crustal uplift, while very rapid regression later occurred during the early Holocene. Anundsen (1985) denoted this event as the Younger Dryas transgression. This phenomenon can be viewed in another way, focusing instead on the extremely rapid uplift occurring in the early Holocene. This event is typical of most of the Norwegian shore-level curves.

Unfortunately, there is very little information about the crustal recovery between 21 000–15 000 years BP. The oldest record of Late Weichselian shore-level displacement in Scandinavia is from Andøya in northern Norway (Vorren 1988) situated within the peripheral part of the former glaciated area. Although this Atlantic island was free of ice by c. 20 000 years BP, uplift did not start until c. 15 000 years BP, and the maximum shore-level displacement did not occur until 13 600 years BP (Vorren 1988). Hence, even though data are scarce for this time interval, it appears that land uplift during the time span 21 000–15 000 years BP may have been negligible. Earlier researchers, e.g. Ahlman (1919), have considered that Andøya, or part of it, was possibly a non-glaciated area during the Weichselian. According to the shore-level data and modelling results, this is very unlikely, since the island would have been covered by relatively thick ice.

Southern Scandinavia lacks uplift data from the earliest part of the latest deglaciation. According to the modelling results, maximum elastic uplift in southern Scandinavia occurred about 14 000 years BP in southern Scandinavia. The existence of the Low Baltic advance and damming of the Baltic Lake may have delayed uplift in this region.

During glaciation, there is an internal redistribution of mantle material to the periphery of the loaded region and growth of a peripheral bulge (Walcott 1972). Deglaciation results in a return-flow of mantle material to the formerly-glaciated region and subsidence of the peripheral bulge. According to the model, the maximum subsidence occurs close to Amsterdam, where subsidence may have been approximately 50 m since the Late Weichselian deglaciation. Further south, subsidence is lower. In northern France the subsidence has been about 10 m.

EUSTATIC DEVELOPMENT

Following deglaciation, the volume of water in the oceans increased in phase with the melting of the ice. This redistribution of water load in the oceans resulted in an effect analogous to the depression of continents by ice-loading. Hydro-isostatic continental levering (Wallcott 1972, Clark et al. 1978, Nakada & Lambeck 1989, Mohrén & Påsse 2001, Douglas & Peltier 2002, Mitrovica & Milne 2002) makes the ocean bottom sink when glacial meltwater enters the ocean, while the continental margins simultaneously tilt upwards as a result of increased ocean-loading following deglaciation. Whitehouse (2009) points out that continental levering is a viscoelastic process that continues for several thousand years following the end of deglaciation. The interaction of sea-level rise and crustal rise has produced a regionally variable shore-level displacement history. This makes it impossible to isolate eustatic changes in non-glaciated areas unless crustal uplift is estimated.

The eustatic curves presented in the literature are constructed using four different methods. Shackelton (1976, 1987) has estimated the amount by which globally averaged sea-level was lower than at present by analysing oxygen isotope dilution histories. This is done on samples of foraminifera from deep-sea sediments. This method has yielded results of importance in establishing long-term records over several glacial cycles. However, it provides very little information about the Holocene eustatic rise.

Secondly corals are used to date shore-level displacement in the sea where crustal changes are assumed to be negligible. This method assumes that shore-level development is identical to eustatic rise. The method is here exemplified in Figure 15 by a curve presented by Peltier & Fairbanks (2006), which is a further development of a curve previously presented by Fairbanks (1989). This "eustatic" curve is constructed from corals collected in the sea off the island of Barbados.

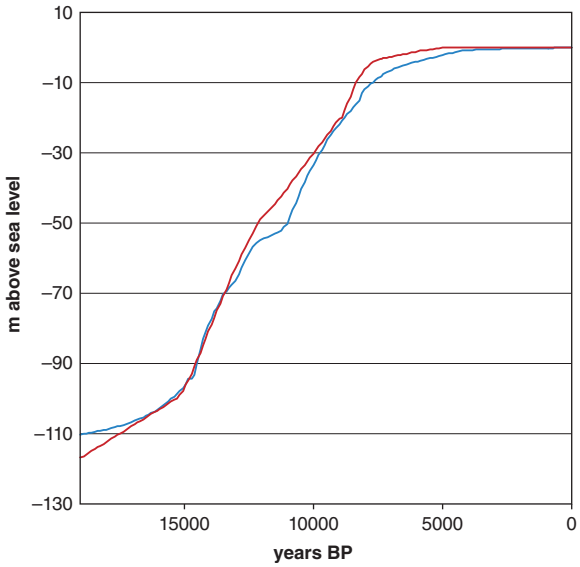

Figure 15. The red curve is an ice-equivalent eustatic sea-level curve derived from prediction of glacial melt water volumes by Peltier (2004). This curve is made to suit the information from eustatic curves derived from coral dates. The blue curve is an example of a coral dated eustatic curve from Barbados (Peltier & Fairbanks 2006).

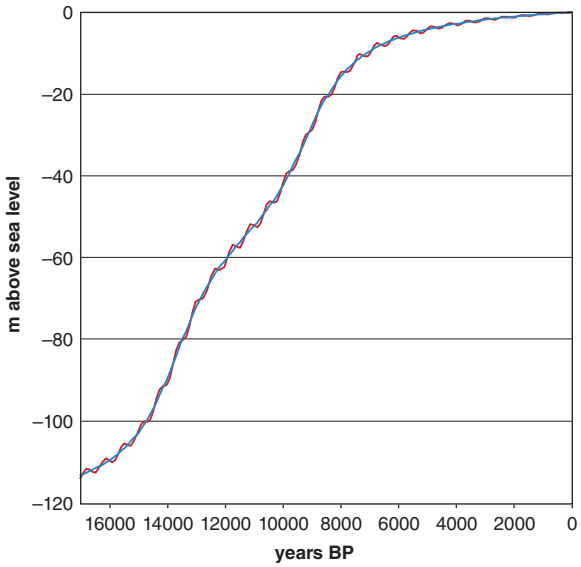

Figure 16. The eustatic development calculated in this model is shown in two ways. The blue curve shows the development calculated using just the main eustatic formula (5). The red curve shows the development when the oscillation formula (6) is added.

A third type of record includes the ice-equivalent eustatic sea-level curves derived from predicting glacial meltwater volumes. Estimates of the global eustatic rise due to the melting of the ice sheets are employed by geophysical modellers, for example by Peltier et al. (1976), Clark et al. (1978), Wu & Peltier (1983), Nakada & Lambeck (1987, 1987), Peltier (1988, 1991, 1994), Flemming et al. (1998) and Bassett et al. (2005). This type of curve is here exemplified by a curve calculated by Peltier (2004) and shown in Figure 15.

The fourth method of making eustatic curves is from shore-level modelling in formerly glaciated areas (Fig. 16). Input data are shore-level curves and modelling results of the crustal movement. This method is used in this paper. One of the advantages of this method is that the abundance of shore-level curves yields high precision data. This is of particular importance for the Holocene development, where the other types of eustatic curves more or less lack empirical information.

The differences between the types of eustatic curves are most obvious in the Holocene (Fig. 17). To understand climate trends and predict future sea-level development, it is of the utmost importance to have reliable knowledge of eustatic changes during the Holocene. Even though the oscillatory factor is of minor importance for overall modelling of Weichselian shore-level displacement, this paper focuses on this, since recent shore-level displacement is strongly associated with an oscillatory sea-level rise.

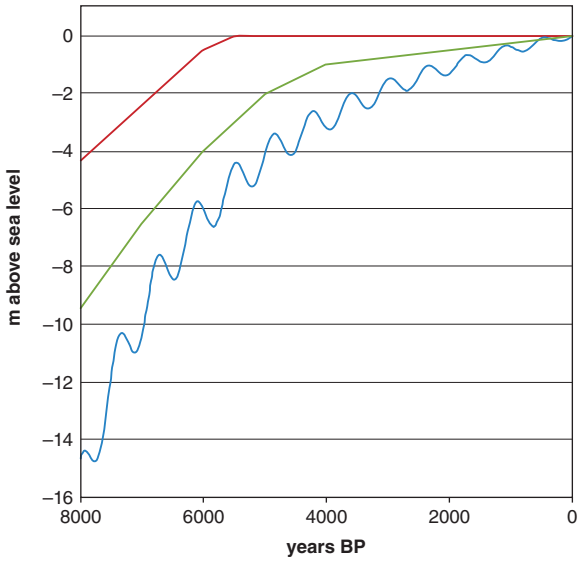

Figure 17. Comparison between the different types of eustatic curves. The red curve is an ice-equivalent eustatic sea-level curve derived from prediction of glacial melt water volumes by Peltier (2004. The green curve is an example of a coral dated eustatic curve from Barbados (Peltier & Fairbanks 2006). The blue curve is the eustatic curve derived in the present model.

Coral-dated and meltwater-calculated curves show significantly higher levels within the Holocene part of eustatic development compared with the modelled eustatic curve. The coral-dated curve is constructed from

very few dates in this part and corals close to the present shore-level have probably been raised by continental levering. The result is that the eustatic levels in these curves have been exaggerated. The eustatic curves derived from predicting glacial meltwater volumes all show very small eustatic changes since c. 8 000 BP, and even no change at all since 5 000 BP. The method of calculating eustatic rise from melting ice volumes is necessarily very insecure and cannot be expected to give any details of eustatic development. There are no empirical data on former ice volumes, and the periods when these volumes were transformed to meltwater are predicted from various coral dating results. The early maximum eustatic development in these curves is derived from the existence of a Holocene highstand at c. 5 000 BP in non-glaciated areas. This highstand appears to match eustatic development, and has convinced many sea-level researchers that there were no eustatic changes during the Middle and Late Holocene. However, this highstand is due to hydro-isostatic continental levering, which means that the eustatic level during the Holocene should be lower than predicted from meltwater curves (Whitehouse 2009).

If we assume a hypothetical coastal area without crustal changes, the shore-level displacement at that place would equal the eustatic rise. This explains why all shore-levels will be found below the eustatic sea-level curve in an area with subsidence, while all shore-levels will be found above the eustatic sea-level curve in an area with crustal uplift. This postulate can be used to test the reliability of eustatic curves. Dated shore-levels from Wismar on the southern Baltic Sea coast from Lampe et al. (2010) can be used as input data from an uplift area in such a test. Data from Holland (Jelgersma 1979) show dated shore-levels from a subsidence area. These dated shore-levels are inserted in Figure 18. This figure also comprises a eustatic curve presented by Lambeck et al. (2010). The test clearly shows that this curve cannot be accepted as a eustatic curve. This is remarkable, since this curve is used by the IPCC to describe sea-level changes.

Eustatic curves constructed from predictions of glacial meltwater volumes do not take into account changes in ice volume due to climatic changes other than the large-scale glacial cycles. However, the eustatic curve derived from modelling shore-level curves shows that there were eustatic fluctuations throughout the Holocene. These fluctuations were due to a continuous process in which Arctic and Antarctic ice volumes change, due to climatic fluctuations. For example, Hjort et al. (1997) have shown that large fluctuations in Antarctic ice occurred as recently as c. 4 500 years BP.

Coral-dated and meltwater-estimated eustatic curves use methods that do not allow detection of small variations in eustatic levels. This shortcoming means that these two types of eustatic curve cannot be used to dispute the oscillations derived within the modelled eustatic curve.

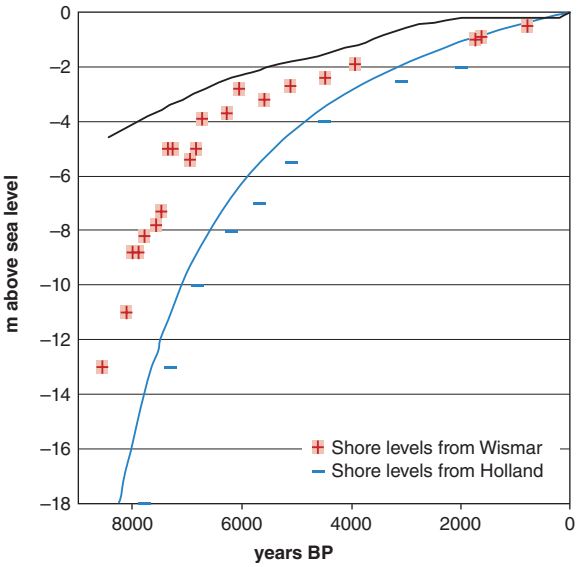

Figure 18. The reliability of the eustatic curve (black) presented by Lambeck et al. (2010) is tested in this figure by inserting shore-level data from a subsidence area (Holland) and shore-level data from an area with crustal uplift (Wismar). Shore levels from Holland (Jelgersma 1979) are shown by blue dots and shore-levels from Wismar in the southern Baltic Sea (Lampe et al. 2010) are shown by red marks. If the eustatic curve was correct the dated shore-levels from Wismar should fall above the eustatic curve, while the shore-levels from Holland should fall below the eustatic curve. As shore-level data from the uplift area fall well below the curve, the test clearly shows that the eustatic curve presented by Lambeck et al. (2010) can't be accepted as a eustatic curve. The shore-level data show that the eustatic rise most probably should have a course similar to the blue curve.

Shifts from regressional to transgressional phases occur when the uplift rate falls below the rate of eustatic rise. These conditions exist particularly in areas with moderate glacial isostatic rise, for example in southern Scandinavia. Because the tidal range is extremely low in this area (<0.2 m), very small changes in eustatic movements can be detected there.

A study of published eustatic curves quickly reveals a widespread scepticism as to the existence of eustatic oscillations. This is remarkable, since changes between transgressions and regressions have been well investigated and scientifically demonstrated by biostratigraphical methods in most of northern Europe for example by Behre (2007), Berglund (1971), Christensen (1993), Digerfeldt (1975), Gembert (1987), Jardine (1975), Lampe et al. (2010), Liljegren (1982), Miller (1982), Mörner (1969, 1976, 1980), Påsse (1983, 1986, 1987, 1988, 1990, 2003), Persson, C. (1979), Persson, G. (1973),

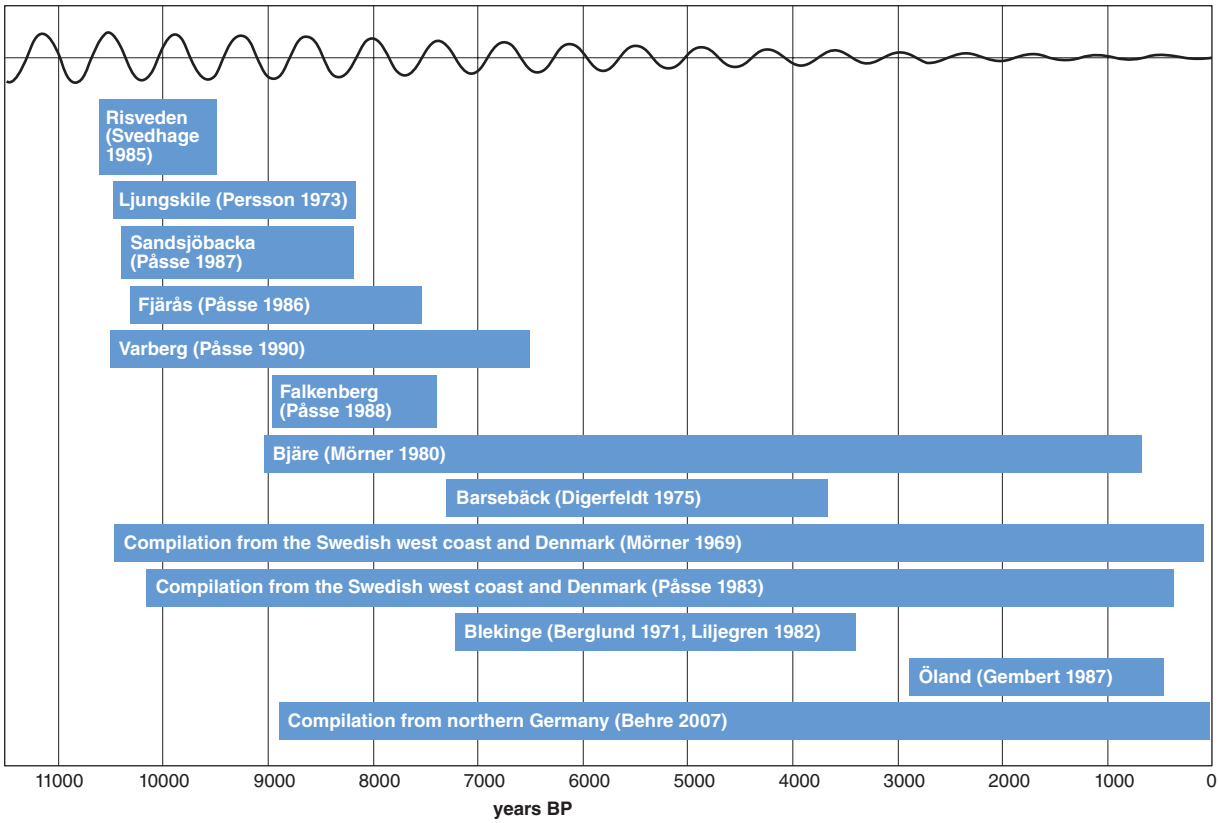

Figure 19. The rectangles represent time intervals for recorded eustatic oscillations at different sites. This compilation shows that oscillations are demonstrated during the whole of Holocene but within different areas at different time intervals. The approximate amplitudes of the oscillations are shown at the top of the figure.

Svedhage (1985) and Tooley (1978). The intervals where these oscillations occurred at different sites are shown in Figure 19. This compilation shows that oscillations are demonstrated throughout the Holocene but at different intervals in different regions.

Figure 20 shows shore-level displacement at Blekinge (Berglund 1971, Liljegren 1982) calculated in two different ways by the present model. In one of the calculations, the shore-level displacement is derived using only the main eustatic development, i.e. by eliminating the oscillatory effect. This calculation gives a good approximation of the shore-level displacement, and the curve could hypothetically have been constructed from the shore-level model presented by Lambeck et al. (1998a). It could even have been drawn by hand. This simplified curve is here shown to explain how easy it is to calculate the oscillations as the amplitudes represent the differences between the simplified modelled shore-level curve and the empirical data. We include this figure to show that the estimation of the amplitude of the oscillations does not depend on our model. The result would be more or less the same even using a curve drawn by hand.

The amplitude of the changes between shore-level transgressions and regression is validated using information about the contemporary crustal movement. The peak amplitude of the oscillation was thus as much as ±1.5 m during early Holocene. Today the amplitude has diminished to around ±20 cm. The oscillations can be traced back at least to c. 10 800 years BP but indications of Late Weichselian oscillations exist. The modelling indicates that the amplitude was largest during the early Holocene and has since declined considerably (Fig. 19). The largest amplitudes occurred when the overall eustatic rise was fastest. That is thus equivalent to the time when the glaciers must have melted most rapidly. Accordingly, the sea-level fell even during warm periods, which indicates that the oscillations are driven by a very strong process.

Oscillation chronology in the shore-level curves is established by radiocarbon dating. The confidence interval of the radiocarbon dating is too large to obtain completely reliable results. However, the main problem in proving whether the oscillations occur regularly is deciding what the dated sediments represent in the cycles.

The assumption that the sea-level has oscillated in cycles of approximately 550 years, i.e. around 275 years between maxima of regression and transgression, has given satisfactory results within the model. The cycles are analysed by making visual comparisons between empirical and modelled shore-level curves. Even if the method is rough, an eventual fault in this assumption is most probably less than ±50 years. As the main eustatic rise is superimposed by oscillatory fluctuation, the main eustatic rise extends the transgression phases to some 325 years, whereas the regression phases are shortened to about 225 years. The relationship between overall eustatic development and oscillatory fluctuations is shown in Figure 21.

PALEOGEOGRAPHICAL MAPS AND VISUALISATION OF SHORE-LEVEL CHANGES

A human lifetime is so short that we usually do not appreciate changes occurring in the landscape. Accordingly, a landscape is considered more or less constant even though the landscape, climate and shore-levels are undergoing constant change. These changes are not always slow and invisible. Shore-level displacement along the northern coast of Sweden is currently one centimetre per year. When humans first arrived in this area, shore-level displacement was 10 cm per year (i.e. one metre every 10 years).

A method of constructing shore-level maps has been developed at the Geological Survey of Sweden. These maps show the former extent of the ice sheet, land and sea, and also how rivers and lakes have changed. The model can calculate the amount of depression at any given date. A grid representing a paleo-DEM (digital elevation model) is calculated by subtracting a calculated download from the present DEM. The DEM used for Swedish inland areas has a grid cell size of 50 × 50 m and comes from the Swedish Land Survey. The DEM used outside Sweden is a Norwegian data set of 1 000 m cell size and a NOAA (National Oceanic and Atmospheric Administration) global grid with 10 km resolution, which was resampled to a cell size of 500 m.

By combining the information of the eustatic level, including the Baltic Ice Lake and the Ancylus Lake levels, and the paleo-DEM, it is a simple logical operation to calculate the shoreline configurations within a GIS program. Ancient lakes can be calculated with a geoprocessing function that fills in sinks in a surface raster. The lakes represent the differences between the filled paleo-DEM and the paleo-DEM. By combining this information with the former ice distribution, it is also possible to model the distributions of glacial lakes at specific times. Drainage patterns can be calculated using standard hydrological functions such as flow direction and streamline.

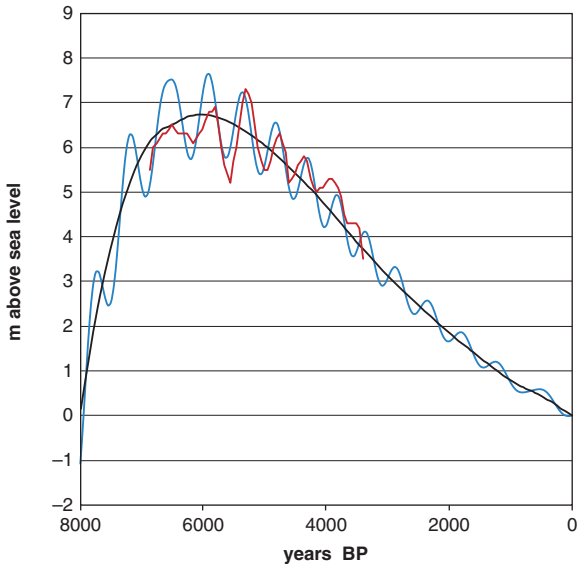

Fig.20. Shore-level curves from Blekinge. The red curve is a unification of two only slightly divergent curves presented by Berglund (1971) and Liljegren (1982). The black curve is the shore-level displacement according to the present model, but where the eustatic oscillations are excluded in the calculation. The blue curve is the modelled curve, when the eustatic oscillations are included in the eustatic development.

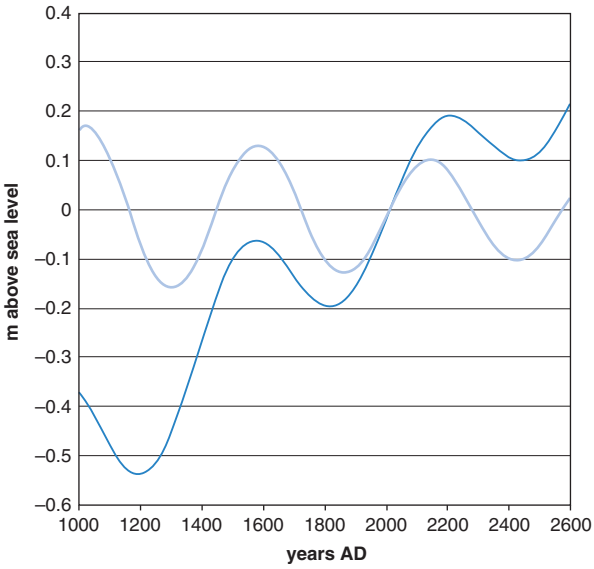

Figure 21. The dark blue curve shows the total eustatic development. The light blue curve shows the oscillations. As the main eustatic rise is superimposed by oscillatory fluctuations, the main eustatic rise extends the transgression phases to c. 325 years, while the regression phases are shortened to c. 225 years.

The present morphology differs from earlier existing morphology not just because of crustal changes, but also due to changes caused by erosional or depositional processes. The present DEM is the basis for calculating a paleo-DEM, which means that the paleo-DEM could contain some flaws due to post-glacial erosion or deposition. This is particularly true if erosion or deposition has changed a threshold site; this may give rise to a serious source of error. However, large changes of elevation due to erosion or deposition are rare and may actually be corrected within the paleo-DEM.

At the Geological Survey of Sweden website (www.sgu.se) it is possible to download both local and regional paleogeographic maps constructed by the model presented here.

Conclusions

The present shore-level model is based solely on empirical shore-level data and is thus not dependent on assumptions about ice thickness, deglaciation rates or geophysical parameters. The main result presented in this paper is the detailed spatial information on shorelines, which provides specific site information as well as data for compiling paleogeographical maps.

The main trend of the maximum uplift is that it occurred in a time-transgressive way following the course of deglaciation. However, there are some exceptions to the main trend. The main uplift within the coastal areas of Norway occurred much later than in the rest of Scandinavia. The west coast of Norway was uplifted at more or less the same time as central northern Sweden. According to data from northern Norway and southern Scandinavia, the uplift in most of Scandinavia did not start until c. 15 000 years BP, and the maximum shore-level displacement did not occur until 14 000 years BP.

Deglaciation results in a return flow of mantle material to the formerly glaciated region and subsidence of the peripheral bulge. According to the model, the maximum subsidence is found close to Amsterdam, where the subsidence may have been approximately 50 m since the Late Weichselian deglaciation.

The model has also made it possible to calculate global eustatic development in detail from shore-level curves and tide-gauge data. Tide-gauge data reveal an ongoing sea-level rise in the order of 1.6 mm/y. Eustatic development is composed of two components: the main eustatic rise and an oscillatory movement, with changes between rises and falls in sea-level. The oscillations occur with a periodicity of about 550 years and are related to changing volumes of glacial ice due to variations in climate. The present ongoing sea-level rise was preceded by about 20 oscillations with similar natures. This regularity shows that the present sea-level rise is most probably due to a natural process.

Acknowledgements

This presentation is a synthesis and a revision of earlier shore-level projects supported jointly by the Swedish Nuclear Fuel and Waste Management CO and the Geological Survey of Sweden. We thank Colby A. Smith for all his suggestions for improving the manuscript.

References

Ahlmann, H.W., 1919: Geomorphological studies in Norway. *Geografiska annaler 1*, 1–48, 193–252.

Ågren, J. & Svensson, R., 2007: Postglacial land uplift model and system definition for the new Swedish height system RH 2000. *Lantmäteriet-Rapport 2007:4*.

Andersen, S., Erikstad, L., Ingólfsson, Ó., Lundqvist, J., Pedersen, S.S., Salonen, V.P., Selonen, O. & Vilborg, L., 1998: Israndlinier i Norden. *Nordiska Ministerrådet Köpenhamn, Tema Nord 1998:584*, 1–372.

Anundsen, K., 1985: Changes in shore-level and ice-front position in Late Weichselian and Holocene, southern Norway. *Norsk Geografisk Tidsskrift 39*, 205–225.

Åse, L.-E., 1970: Kvartärbiologiska vittnesbörd om strandförskjutningen vid Stockholm under de senaste c. 4000 åren. *Geologiska Föreningens i Stockholm Förhandlingar 92*, 49–78.

Bassett, S.E., Milne, G.A., Mitrovica, J.X. & Clark, P.U., 2005: Ice sheet and solid earth influences on far-field sea-level histories. *Nature 309*, 925–928.

Behre, K.-E., 2007: A new sea-level curve for the southern North Sea. *Boreas 36*, 82–102.

Bennike, O. & Jensen, J.B., 1995: Near-shore Baltic ice lake deposits in Fakse Bugt, southeast Denmark. *Boreas 24*, 185–195.

Bennike, O., Jensen, J.B., Lemke, W., Kuijpers, A. & Lomholt, S., 2004: Late- and postglacial history of the Great Belt, Denmark. *Boreas 33*, 18–33.

Berglund, B., 1971: Littorina transgressions in Blekinge, south Sweden. A preliminary survey. *Geologiska Föreningens i Stockholm Förhandlingar 93*, 625–652.

Berglund, M., 1995: The Late Weichselian deglaciation, vegetational development and shore displacement in Halland, southwestern Sweden. *University of Lund, Department of Quaternary Geology Thesis 35*, 1–113.

Berglund, M., 2004: Holocene shore displacement and chronology in Ångermanland, eastern Sweden, the Scandinavian glacio-isostatic centre. *Boreas 33*, 48–60.

Berglund, M., 2005: The Holocene shore displacement of Gästrikland, eastern Sweden: a contribution to the knowledge of Scandinavian glacio-isostatic uplift. *Journal of Quaternary Science 20:6*, 519–531.

Berglund, M., 2010: Litorina Sea shore displacement and pollen analytical indications of forest succession during the Mid-Holocene in Gästrikland, east central Sweden. *GFF 132*, 213–226.

Bird, E.C.F. & Klemsdal, T., 1986: Shore displacement and the origin of the lagoon at Brusand, southwestern Norway. *Norsk Geografisk Tidsskrift 40*, 27–35.

Björck, S., 1979: Late Weichselian stratigraphy of Blekinge, SE Sweden, and water level changes in the Baltic Ice Lake. *University of Lund, Department of Quaternary Geology Thesis 7*, 1–248.

Björck, S. & Digerfeldt, G., 1982: Late Weichselian shore displacement at Hunneberg, southern Sweden, indicating complex uplift. *Geologiska Föreningens i Stockholm Förhandlingar 104*, 132–155.

Björck, S. & Digerfeldt, G., 1986: Late Weichselian – Early Holocene shore displacement west of Mt. Billingen, within the Middle Swedish end-moraine zone. *Boreas 15*, 1–18.

Björck, S. & Digerfeldt, G., 1991: Alleröd–Younger Dryas sea-level changes in southwestern Sweden and their relation to the Baltic Ice Lake development. *Boreas 20*, 115–133.

Björck, S. & Möller, P., 1987: Late Weichselian environmental history in southeastern Sweden during the deglaciation of the Scandinavian ice sheet. *Quaternary Research 28*, 1–37.

Brunnberg, L., Miller, U. & Risberg, J., 1985: Project eastern Svealand: development of the Holocene landscape. *Iskos 5*, 85–91.

Caldenius, C. & Linnman, G., 1949: En senkvartär regressions- och transgressionslagerföljd vid Halmstad. *Sveriges geologiska undersökning C 502*, 1–26.

Caldenius, C., Larsson, W., Mohrén, E., Linnman, G. & Tullström, H., 1966: Beskrivning till kartbladet Halmstad. *Sveriges geologiska undersökning Aa 198*, 1–138.

Cato, I., 1992: Shore displacement data based on lake isolations confirm the postglacial part of the Swedish geochronological time scale. *Sveriges geologiska undersökning Ca 81*, 75–80.

Cathles, L.M., 1975: *The viscosity of the earth's mantle*. Princeton University Press, Princeton, New Jersey, 1–386.

Clark, R.D., Farrell, W.E. & Peltier, W.R., 1978: Global changes in postglacial sea-level: a numerical calculation. *Quaternary Research 9*, 265–278.

Christensen, C., 1993: Land and sea. *In* S. Hvass & B. Stovgaard (eds.): *Digging into the past – 25 years of Archaeology in Denmark*. Aarhus Universitetsforlag, 20–23.

Church, J.A., 2001: Changes in sea-level. *In* J.T. Houghton (ed.): *Climate Change 2001: The scientific basis. Contribution of Working group I to the third assessment report of the Intergovernmental panel on climate change*. Cambridge University Press, Cambridge, United Kingdom and New York, 639–693.

Clemmensen, L.B., Richardt, N. & Andersen C., 2001: Holocene sea-level variation and spit development: data from Skagen Odde, Denmark. *The Holocene 11:3*, 323–331.

Daly, R.A., 1934: *The changing world of the ice age*. Hafner, New York, 1–271.

Digerfeldt, G., 1975: A standard profile for Littorina transgression in western Skåne, South Sweden. *Boreas 4*, 125–142.

Dolukhanov, P.M., 1979: The Quaternary History of the Baltic. Leningrad and Soviet Carelia. *In* V. Gudelis & L.-K. Königsson (eds.): The Quaternary history of the Baltic. *Acta Universitatis Upsaliensis Symposia Universitatis Upsaliensis Annum Quingentesimum Celebrantes 1*, 115–125.

Douglas, B.C. & Peltier, W.R., 2002: The puzzle of global sea-level rise. *Physics Today 55*, 35–40.

Ekman, M., 1996: A consistent map of the postglacial uplift of Fennoscandia. *Terra Nova 8*, 158–165.

Ekman, M., 2000: Determination of global sea-level rise and its change with time. *Small Publications in Historical Geophysics 7*, 1–20.

Emery, K.O. & Aubrey, D.G., 1991: *Sea-levels, land levels, and tide gauges*. Springer-Verlag, 237 pp.

Eronen, M., 1976: A radiocarbon-dated Ancylus transgression site in south-eastern Finland. *Boreas 5*, 65–76.

Eronen, M., 1983: Late Weichselian and Holocene shore displacement in Finland. *In* D.E. Smith & G. Dawson (eds.): Shorelines and isostacy. *Institute of British Geographers, Special Publication 16*, 183–207.

Eronen, M. & Haila, H., 1982: Shorelines displacement near Helsinki, southern Finland, during the Ancylus Lake stage. *Annales Academiae Scientiarum Fennicae AIII 134*, 111–129.

Eronen, M., Glückert, G., van de Plassche, O., van der Plicht, J. & Rantala, P., 1995: Land uplift in the Olkiluoto-Pyhäjärvi area, southwestern Finland, during the last 8,000 years. *Nuclear Waste Commission of Finnish Power Companies, Report YJT-95-17*, 1–26.

Fairbanks, R.G., 1989: A 17,000-years glacio-eustatic sea-level record: influence of glacial melting rates on the Younger Dryas event and deep- ocean circulation. *Nature 342*, 637–642.

Flemming, K., Johnston, P., Zwartz, D., Yokoyama, Y., Lambeck, K. & Chappell, J., 1998: Refining the eustatic sea-level curve since the Late Glacial Maximum using far- and intermediate-field sites. *Earth and Planetary Science Letters 163*, 327–342.

Fjeldskaar, W., 1994: Viscosity and thickness of the astenosphere detected from Fennoscandian uplift. *Earth and Planetary Science Letters 126*, 399–410.

Fjeldskaar, W., 2000: How important are elastic deflections in the Fennoscandian postglacial uplift? *Norsk Geologisk Tidsskrift 80*, 57–62.

Fjeldskaar, W. & Cathles, L., 1991: The present rate of uplift of Fennoscandia implies a low-viscosity astenosphere. *Terra Nova 3*, 393–400.

Gehrels, W.R., Szkornik, K., Bartholdy, J., Kirby, J.R., Bradley, S.L., Marshall, W.A., Heinemeier, J. & Pedersen, J.B.T., 2006: Late Holocene sea-level changes and isostasy in western Denmark. *Quaternary Research 66*, 288–302.

Gembert, B., 1987: Sedimentological studies of a beach ridge system in Ottenby, Öland, South-eastern Sweden and related sea-level changes in the Baltic basin. *Striae 27*, 1–66.

Glückert, G., 1976: Post-glacial shore-level displacement of the Baltic in SW Finland. *Annales Academiae Scientiarum Fennicae AIII 134*, 1–92.

Glückert, G., 1978: *Östersjöns postglaciala strandförskjutning och skogens historia på Åland*. Publication Department of Quaternary Geology, University of Turku, 1–106.

Glückert, G. & Ristaniemi, O., 1982: The Ancylus transgression west of Helsinki, South Finland – a preliminary report. *Annales Academiae Scientiarum Fennicae AIII 134*, 99–134.

Hafsten, U., 1983: Shore-level changes in South Norway during the last 13,000 years, traced by biostratigraphical methods and radiometric datings. *Norsk Geografisk Tidsskrift 37*, 63–79.

Hald, M. & Vorren, T.O., 1983: A shore displacement curve from the Tromsö district, North Norway. *Norsk Geologisk Tidsskrift 63*, 103–110.

Hedenström, A. & Risberg, J., 1999: Early Holocene shore-displacement in southern central Sweden as recorded in elevated isolated basins. *Boreas 28*, 490–504.

Hedenström, A. & Risberg, J., 2003: Shore displacement in northern Uppland during the last 6500 calendar years. *Swedish Nuclear Fuel and Waste Management Co SKB Technical Report 03-17*, 1–48.

Hedenström, A., 2001: Early Holocene shore displacement in eastern Svealand, Sweden, based on diatom stratigraphy, radiocarbon chronology and geochemical parameters. *Stockholm University, Quaternaria Ser. A, Theses and Reaserch Papers 10,* 1–36.

Helle, S.K., Anundsen, K., Aasheim, S. & Hafildason, H., 1997: Indications of a younger Dryas marine transgression in inner Hardanger, West Norway. *Norsk Geologisk Tidsskrift 77*, 101–117.

Hjort, C., Ingólfsson, Ó., Möller, P. & Lirio, J.M., 1997: Holocene glacial history and sea-level changes on James Ross Island, Antarctic Peninsula. *Journal of Quaternary Science 12*, 259–273.

Hyvärinen, H., 1980: Relative sea-level changes near Helsinki, southern Finland during early Litorina times. *Bulletin of the Geological Society of Finland 52*, 207–219.

Hyvärinen, H., 1984: The Mastogloia stage in the Baltic Sea history: Diatom evidence from southern Finland. *Bulletin of the Geological Society of Finland 56*, 1–2 & 99–115.

Jardine, W.G., 1975: Chronology of Holocene marine transgression and regression in south-western Scotland. *Boreas 4*, 173–196.

Jelgersma, S., 1979: Sea-level changes in the North Sea basin. *In* E. Oele, R.T.E. Schüttenhelm & A.J. Wiggers (eds.): The Quaternary history of the North Sea. *Acta Universitatis Upsaliensis Symposia Universitatis Upsaliensis Annum Quingentesimum Celebrantes 1*, 233–248.

Jensen, J.B., Bennike, O., Witkowski, A., Lemke, W. & Kuijpers, A., 1999: Early Holocene history of the southwestern Baltic Sea: the Ancylus Lake stage. *Boreas 28*, 437–453.

Kabailiene, M., 1997: Shoreline displacement, palaeoecological conditions and human impact on the southeastern coast of Baltic sea. *In* A. Grigelis. (ed.): *The fifth marine geological conference "The Baltic"*. Lihuanian Institute of Geology. Vilnius. 114–122.

Kaland, P.E., 1984: Holocene shore displacement and shorelines in Hordaland, western Norway. *Boreas 13*, 203–242.

Kaland, P.E., Krzywinski, K. & Stabell, B., 1984: Radiocarbon dating of the transitions between marine and lacustrine sediments and their relation to the development of lakes. *Boreas 13*, 243–258.

Kessel, H. & Raukas, A., 1979: The Quaternary history of the Baltic, Estonia. *In* V. Gudelis & L.-K. Königsson (eds.): The Quaternary history of the Baltic. *Acta Universitatis Upsaliensis Symposia Universitatis Upsaliensis Annum Quingentesimum Celebrantes 1,* 127–146.

Kjemperud, A., 1986: Late Weichselian and Holocene shore displacement in the Trondheimsfjord area, central Norway. *Boreas 15*, 61–82.

Klug, H., 1980: Der Anstieg des Ostseespiegels im deutchen Küstenraum set dem Mittelatlantikum. *Eiszeitalter und Gegenwart 30*, 237–252.

Korhola, A., 1995: The Littorina transgression in the Helsinki region, southern Finland: new evidence from coastal mire deposits. *Boreas 24*, 173–183.

Krzywinski, K. & Stabell, B., 1984: Late Weichselian sea-level changes at Sotra, Hordaland, western Norway. *Boreas 13*, 159–202.

Lambeck, K., 1991: A model for Devensian and Flandrian glacial rebound and sea-level change in Scotland. *In* R. Sabadini, K. Lambeck & E. Boschi. (eds): *Glacial isostasy, sea-level and mantle rheology.* Kluwer Academic Publishers, 33–61.

Lambeck, K., 1997: Sea-level change along the French Atlantic and Channel coasts since the time of the Last Glacial Maximum. *Palaeogeography, Palaeoclimatology, Palaeoecology 129*, 1–22.

Lambeck, K., 1999: Shoreline displacement in southern Sweden and the evolution of the Baltic Sea since the last maximum glaciation. *Journal of the Geological Society 156*, 465–486.

Lambeck, K., Smither, C. & Johnston, P., 1998a: Sea-level change, glacial rebound and mantle viscosity for northern Europe. *Geophysical Journal International 134*, 102–144.

Lambeck, K., Smither, C., Ekman, M., 1998b: Test of glacial rebound models for Fennoscandia based on instrumented sea- and lake-level records. *Geophysical Journal International 135*, 375–387.

Lambeck, K., Woodroffe, C.D., Antonioli, F., Anzidei, M., Gehhrels, W.R., Laborel, J. & Wright, A.J., 2010: Paleoenvironmental records, geophysical modelling, and reconstruction of sea-level trends and variability on centennial longer timescales. *In* J.A. Church, P.L. Woodworth, T. Aarup & W.S. Wilson (eds.): *Understanding sea-level rise and variability*. Wiley-Blackwell, 61–121.

Lampe, R., Endtmann, E., Janke, W. & Meyer, H., 2010: Relative sea-level development and isostasy along the NE German Baltic Sea coast during the past 9 ka. *Quaternary Science Journal 59*, 3–20.

Liljegren, R., 1982: Paleoekologi och strandförskjutning i en Littorinavik vid Spjälkö i mellersta Blekinge. *University of Lund, Department of Quaternary Geology, Thesis 11*, 1–95.

Lindén, M., Möller, P., Björck, S. & Sandgren, P., 2006: Holocene shore displacement and deglaciation chronology in Norrbotten, Sweden. *Boreas 35*, 1–22.

Lisitzin, E., 1974: *Sea-level changes*. Elsevier Scientific Publishing Co. 286 pp.

Lohne, Ø.S., Bondevik, S., Mangerud, J. & Svendsen, J.I., 2007: Sea-level fluctuations imply that the Younger Dryas ice-sheet expansion in western Norway commenced during the Allerød. *Quaternary Science Reviews 26*, 2128–2151.

Lundqvist, G., 1962: Geological radiocarbon datings from the Stockholm station. *Sveriges geologiska undersökning C 589*, 1–23.

Lundqvist, J., 1994: Inlandsisens avsmältning. *In* C. Fredén (ed.): *Berg och Jord*, *Sveriges Nationalatlas*. 124–135.

Lundqvist, J. & Wohlfarth, B., 2001: Timing and east-west correlation of south Swedish ice marginal lines

during the Late Weichselian. *Quaternary Science Reviews 20*, 1127–1148.

McConnell, R.K., 1968: Viscosity of the Mantle from Relaxation Time Spectra of Isostatic Adjustment. *Journal of Geophysical Research 73*, 7089–7105.

Miller, U. & Robertsson, A.-M., 1982: The Helgeandsholmen excavation: An outline of biostratigraphical studies to document shore displacement and vegetational changes. *Council of Europe Study Group PACT Journal 7*, 311–327.

Miller, U. & Robertsson, A.-M., 1988: Late Weichselian and Holocene environmental changes in Bohuslän, Southwestern Sweden. *Geographia Polonica 55*, 103–111.

Midtbø, I., Prøsch-Danielsen, L. & Helle, S.K., 2000: Den Holocene (etteristidens) strandlinje i området Mandal-Kristiansand, Vest-Agder, Sør-Norge: Et forprojekt. *Arkeologisk museum i Stavanger, AmS-Varia 37*, 37–49.

Mitrovica, J.X. & Milne, G.A., 2002: On the origin of late Holocene sea-level highstands within equatorial ocean basins. *Quaternary Science Reviews 21,* 2179–2190.

Møller, J.J., 1984: Holocene shore displacement at Nappstraumen, Lofoten, North Norway. *Norsk Geologisk Tidsskrift 64*, 1–5.

Møller, J.J., 2003: Late Quaternary sea-level and coastal settlement in the European north. *Journal of Coastal Research 19*, 731–737.

Morén, L. & Påsse, T., 2001: Climate and shoreline in Sweden during Weichsel and the next 150,000 years. *Swedish Nuclear Fuel and Waste Management Co, SKB Technical Report 01-19*, 1–67.

Mörner, N.-A., 1969: The Late Quaternary history of the Kattegatt sea and the Swedish west coast. S*veriges geologiska undersökning C 640*, 1–487.

Mörner, N.-A., 1976: Eustatic changes during the last 8,000 years in view of radiocarbon calibration and new information from the Kattegatt region and other northwestern European coastal areas. *Palaeogeography, Palaeoclimatology, Palaeoecology 19*, 63–85.

Mörner, N.-A., 1977: Past and present uplift in Sweden glacial isostasy, tectonism and bedrock influence. *Geologiska Föreningens i Stockholm Förhandlingar 99*, 48–54.

Mörner, N.-A., 1980: The Northwest European "sea-level laboratory" and regional Holocene eustasy. *Palaeogeography, Palaeoclimatology, Palaeoecology 29*, 281–300.

Nakada, M. & Lambeck, K., 1987: Glacial rebound and relative sea-level variations: a new appraisal. *Geophysical Journal Royal Astronomical Society 90*, 171–224.

Nakada, M. & Lambeck, K., 1989: Late Pleistocene and Holocene sea-level change in the Austrailian region and mantle rheology. *Geophysical Journal 96*. 497–517.

Nakiboglu, S.M. & Lambeck, K., 1991: Secular sea-level change. *In* R. Sabadini, K. Lambeck & E. Boschi (eds.): *Glacial isostasy, sea-level and mantle rheology*. Kluwer Academic Publishers, 237–258.

Nansen, F., 1922: The strandflat and isostasy. *Christiania Videnskapliga Selskaps Skrifter 1921(11),* 1–315.

Påsse, T., 1983: Havsstrandens nivåförändringar i norra Halland under holocen tid. *Göteborgs universitet. Geologiska institutionen A 45*, 1–174.

Påsse, T., 1986: Beskrivning till jordartskartan Kungsbacka SO. *Sveriges geologiska undersökning Ae 56*, 1–106.

Påsse, T., 1987: Shore displacement during the Late Weichselian and Holocene in the Sandsjöbacka area, SW Sweden. *Geologiska Föreningens i Stockholm Förhandlingar 109*, 197–210.

Påsse, T., 1988: Beskrivning till jordartskartan Varberg SO/Ullared SV. *Sveriges geologiska undersökning Ae 86*, 1–98.

Påsse, T., 1990a: Emperical estimation of isostatic uplift using the lake-tilting method at Lake Fegen and at Lake Säven, southwestern Sweden. *Mathematical Geology 22(7)*, 803–824.

Påsse, T., 1990b: Beskrivning till jordartskartan Varberg NO. *Sveriges geologiska undersökning Ae 102*, 1–117.

Påsse, T., 1996a: A mathematical model of the shore-level displacement in Fennoscandia. *Swedish Nuclear Fuel and Waste Management Co, SKB Technical Report 96-24*, 1–92.

Påsse, T., 1996b: Lake-tilting investigations in southern Sweden. *Swedish Nuclear Fuel and Waste Management Co, SKB Technical Report 96-10*, 1–34.

Påsse, T., 1997: A mathematical model of past, present and future shore-level displacement in Fennoscandia. *Swedish Nuclear Fuel and Waste Management Co, SKB Technical Report 97-28*, 1–55.

Påsse, T., 1998: Lake-tilting, a method for estimation of isostatic uplift. *Boreas 27*, 69–80.

Påsse, T., 2001: An empirical model of glacio-isostatic movements and shore-level displacement in Fennoscandia. *Swedish Nuclear Fuel and Waste Management Co, SKB R-01-41*, 1–59.

Påsse, T., 2003: Strandlinjeförskjutning i norra Bohuslän under holocen. *In* P. Person (ed.): *Strandlinjer och vegetationshistoria. Kvartärgeologiska undersökningar inom Kust till kust projektet, 1998–2002*, 33–88.

Påsse, T. & Andersson, L., 2005: Shore-level displacement in Fennoscandia calculated from empirical data. *GFF 127*, 253–268.

Påsse, T. & Daniels, J., 2011: Comparison between a new and an old semi-empirical Fennoscandian shore-level model. *I* A.T.K. Ikonen & T. Lipping (eds.) Proceedings of a seminar on sea-level displacement and bedrock uplift, 10–11 June 2010, Pori, Finland. *Posiva Working Report July 2011*, 47–50.

Peltier, W.R., 1974: The impulse response of Maxwell earth. *Reviews of Geophysics 12*, 649–669.

Peltier, W.R., 1976: Glacial isostatic adjustments – II: The inverse problem. *Geophysical Journal Royal of the Astronomical Society 46*, 605–646.

Peltier, W.R. & Andrews, J.T., 1976: Glacial isostatic adjustments – I: Forward Problem. *Geophysical Journal Royal of the Astronomical Society 46,* 605–646.

Peltier, W.R., 1988: Lithospheric thickness, Antarctic deglaciation history, and ocean basin discretization effect in a global model of postglacial sea-level changes: a summary of some sources of nonuniqueness. *Quaternary Reaserch 29*, 93–112.

Peltier, W.R., 1991: The ICE-3G model of late Pleistocene deglaciation: construction, verification, and applications. *In* R. Sabadini, K. Lambeck & E. Boschi (eds.): *Glacial isostasy, sea-level and mantle rheology*. Kluwer, Dordrecht, 95–119.

Peltier, W.R., 1994: Ice age paleotopography. *Science 265*, 195–201.

Peltier, W.R., 2004: Global glacial isostasy and the surface of the ice-age earth: The ice-5G (VM2) model and GRACE. *Annual Review of Earth and Planetary Science 32*, 111–149.

Peltier, W.R. & Fairbanks, R., 2006: Global glacial ice volume and Last Glacial Maximum duration from an extended Barbados sea-level record. *Quaternary Science Reviews 25*, 3322–3337.

Persson, C., 1979: Shore displacement during Ancylus time in the Rejmyra area, south central Sweden. *Sveriges geologiska undersökning C 755*, 1–23.

Persson, G., 1962: En transgressionslagerföljd från Limhamn. *Geologiska Föreningens i Stockholm Förhandlingar 84*, 47–55.

Persson, G., 1973: Postglacial transgressions in Bohuslän, Southwestern Sweden. *Sveriges geologiska undersökning C 684*, 1–47.

Ramfjord, H., 1982: On the Late Weichselian and Flandrian shoreline displacement in Naeröy, Nord-Tröndelag, Norway. *Norsk Geologisk Tidsskrift 62*, 191–205.

Renberg, I. & Segerström, U., 1981: The initial points on a shoreline displacement curve for southern Västerbotten, dated by varve-counts of lake sediments. *Striae 14*, 174–176.

Richardt, N., 1996: Sedimentological examination of the Late Weichselian sea-level history following deglaciation of northern Denmark. *Geological Society Special Publication 111*, 261–273.

Ringberg, B., 1989: Upper Late Weichselian lithostratigraphy in western Skåne, southernmost Sweden. *Geologiska Föreningens i Stockholm Förhandlingar 111*, 319–337.

Risberg, J., 1991: Palaeoenvironment and sea-level changes during the early Holocene on the Södertörn peninsula, Södermanland, eastern Sweden. *Stockholm University, Department of Quaternary Research Report 20*, 1–27.

Risberg, J., Sandgren, P. & Andrén E., 1996: Early Holocene shore displacement and evidence of irregular isostatic uplift northwest of lake Vänern, western Sweden. *Journal of Paleolimnology 15*, 47–63.

Robertsson, A.-M., 1991: Strandförskjutningen i Eskilstunatrakten för ca 9000 till 4000 år sedan. *Sveriges geologiska undersökning Rapporter och meddelanden 67*, 1–27.

Romundset, A., Lohne, Ø. S., Mangerud, J. & Svendsen, J.I., 2010: The first Holocene relative sea-level curve from the middle part of Hardangerfjorden, western Norway. *Boreas 39*, 87–104.

Rosentau, A., Vassiljev, J., Hang, T., Saarse, V. & Kalm, V., 2008: Development of the Baltic Ice Lake in the eastern Baltic. *Quaternary International 206*, 16–23.

Saarnisto, M., 1981: Holocene emergence history and stratigraphy in the area north of the Gulf of Bothnia. *Annales Academiae Scientiarum Fennicae AIII 130*, 1–42.

Salomaa, R., 1982: Post-glacial shoreline displacement in the Lauhanvuori area, western Finland. *Annales Academiae Scientiarum Fennicae AIII 134*, 81–97.

Salomaa, R. & Matiskainen, H., 1983: Rannan siirtyminen ja arkeologinen kronologia Etelä-Pohjanmaalla. Arkeologian päivät 7 -8.4. *1983 Lammin Biolog. tutkimusasemalla. Karhunhammas 7*, 21–36.

Salonen, V.-P., Räsenen, M. & Terho, A., 1984: Palaeolimnology of ancient Lake Mätäjärvi. Third Nordic Conference on the application of scientific methods in archaeology. Mariehamn, Åland, Finland, 8–11. October 1984. *Iskos 5*, 233–288.

Shackelton, N.J., 1967: Oxygen isotope analyses and Pleistocene temperature readdressed. *Nature 215*, 15–17.

Shackelton, N.J., 1987: Oxygen isotopes, ice volume and sea-level. *Quaternary Science Reviews 6*, 183–190.

Snyder, J.A., Korsun, S.A. & Forman, S.L., 1996: Postglacial emergence and Tapes transgression, north-central Kola Penisula, Russia. *Boreas 25*, 47–56.

Solem, T. & Solem, J., 1997: Shoreline displacement on the coast of Sør-Trøndelag and Møre og Romsdal, Central Norway; a botanical and zoological approach. *Norsk Geologisk Tidsskrift 77*, 193–203.

Stabell, B., 1980: Holocene shorelevel displacement in Telemark, southern Norway. *Norsk Geologisk Tidsskrift 60*, 71–81.

Svedhage, K., 1985: Shore displacement during Late Weichselian and Early Holocene in the Risveden area, SW Sweden. *Göteborgs universitet, Geologiska institutionen A 51*, 1–111.

Sveian, H. & Olsen, L., 1984: En strandforsyvningskurve fra Verdalsøra, Nord-Trøndelag. *Norsk Geologisk Tidsskrift 64*, 27–38.

Svendsen, J.I. & Mangerud, J., 1990: Sea-level changes and pollen stratigraphy on the outer coast of Sunnmøre, western Norway. *Norsk Geologisk Tidsskrift 70*, 111–134.

Svensson, N.-O., 1989: Late Weichselian and Early Holocene shore displacement in the Central Baltic, based on stratigraphical and morphological records from Eastern Småland and Gotland, Sweden. *Lund University, Department of Quaternary Geology 25*, 1–195.

Sørensen, R., 1979: Late Weichselian deglaciation in the Oslofjord area, south Norway. *Boreas 8*, 241–246.

Sørensen, R., 1999: En 14C datert og dendrokronologisk kalibrert strandforskyvningkurve for søndre østfold, Sørøst-Norge. *Arkeologisk museum i Stavanger AmS-Rapport 12 A*, 227–242.

Sørensen, R., Høeg, H.I., Henningsmoen, K.E., Skog, G., Labowsky, S.F. & Stabell, B., 2012: Utviklingen av det senglasiale og tidlig preboreale landskapet og vegetasjonen omkring steinalderboplassene ved Pauler, Larvik kommune, Vestfold. *I* L. Jaksland (ed.): E18 Brunlanesprosjektet, Bind I, Forutsetninger og sammenstilling. *Kulturhistorisk museum, Fornminneseksjonen, Universitetet i Oslo Varia 79*.

Thomsen, H., 1981: Late Weichselian shore-level displacement on Nord-Jæren, south-west Norway. *Geologiska Föreningens i Stockholm Förhandlingar 103*, 447–468.

Tooley, M., 1978: Interpretation of Holocene sea-level changes. *Geologiska Föreningens i Stockholm Förhandlingar 100*, 203–212.

Uscinowicz, S., 2003: Relative sea-level changes, glacial rebound and shoreline displacement in the southern Baltic. *Polish Geological Institute Special papers 10*.

Walcott, R.I., 1972: Past sea-levels, eustasy and deformation of the earth. *Quaternary Research, 2*, 1–14.

Whitehouse, P., 2009: Glacial isostatic adjustment and sea-level change. *Swedish Nuclear Fuel and Waste Management Co, SKB Technical Report 09-11*, 1–105.

Winn, K., Averdieck, F.R., Erlenkeusser, H. & Werner, F., 1986: Holocene sea-level rise in western Baltic and the question of isostatic subsidence. *Meyniana 38*, 61–80.

Woodworth, P.L. & Player, R., 2003: The permanent service for mean sea-level: an update to the 21st century. *Journal of Coastal Research 19*, 287–295.

Vorren, K.-D. & Moe, D., 1986: The early Holocene climate and sea-level changes in Lofoten and Vesterålen, North Norway. *Norsk Geologisk Tidsskrift 66*, 135–143.

Vorren, T., Vorren, K.-D., Alm T., Gulliksen, S. & Lövlie, R., 1988: The last deglaciation (20,000 to 11,000 B.P.) on Andøya, northern Norway. *Boreas 17*, 41–77.

Vuorela, A., Penttinen, T. & Lahdenperä, A.-M., 2009: Review of Bothnian Sea shore-level displacement data and use of a GIS tool to estimate isostatic uplift. *Posiva working report 2009–17*.

Wu, P. & Peltier, W.R., 1983: Glacial isostatic adjustment and the free air gravity anomaly as a constraint on deep mantle viscosity. G*eophysical Journal Royal Astronomical Society 74*, 377–450.

Yu, S.-Y., Berglund, B.E., Andrén, E. & Sandgren, P., 2004: Mid-Holocene Baltic Sea transgression along the coast of Blekinge, SE Sweden – ancient lagoons correlated with beach ridges. *GFF 126*, 257–272.

Geological Survey of Sweden
Box 670
SE-751 28 Uppsala
Phone: +46 18 17 90 00
Fax: +46 18 17 92 10
www.sgu.se

Uppsala 2015
ISSN 0349-2176
ISBN 978-91-7403-291-8
Tryck: Elanders Sverige AB